

Practical Kernel Tests of Conditional Independence

Roman Pogodin

McGill University and Mila

RMN.POGODIN@GMAIL.COM

Antonin Schrab

*Gatsby Computational Neuroscience Unit, University College London
Centre for Artificial Intelligence, University College London*

A.SCHRAB@UCL.AC.UK

Yazhe Li

*Microsoft AI**

YAZHELI@OUTLOOK.COM

Danica J. Sutherland

University of British Columbia and Amii

DSUTH@CS.UBC.CA

Arthur Gretton

*Gatsby Computational Neuroscience Unit, University College London
Google DeepMind*

ARTHUR.GRETTON@GMAIL.COM

Abstract

We describe a data-efficient, kernel-based approach to statistical testing of conditional independence. A major challenge of conditional independence testing is to obtain the correct test level (the specified upper bound on the rate of false positives), while still attaining competitive test power. Excess false positives arise due to bias in the test statistic, which is in our case obtained using nonparametric kernel ridge regression. We propose SplitKCI, an automated method for bias control for the Kernel-based Conditional Independence (KCI) test based on data splitting. We show that our approach significantly improves test level control for KCI without sacrificing test power, both theoretically and for synthetic and real-world data.

Keywords: conditional independence testing, statistical testing, debiasing, type I error control, kernel methods

1 Introduction

Conditional independence (CI) testing is a fundamental problem in statistics: given a confounder C , are two random variables A and B dependent? Applications include basic scientific questions (“is money associated with self-reported happiness, controlling for socioeconomic status?”); evaluating the fairness of machine learning methods (the popular *equalized odds* criterion (Hardt et al., 2016) checks that predictions are independent of a protected status, given the true label); causal discovery (where conditional independence testing is a core sub-routine of many causal structure discovery methods, building on the PC algorithm (Spirtes et al., 2000; Pearl, 2000; Sun et al., 2007; Tillman et al., 2009)), and more. If C takes on a small number of discrete values and sufficient data points are available, the problem can be essentially reduced to unconditional independence testing for each C value. Often, however, C takes on continuous values and/or has complex structure; it is then a major challenge to determine how to “share information” across similar values of C , without making strong assumptions about the form of dependence among the variables.

In simple settings, for instance if (A, B, C) are jointly Gaussian, conditional independence can be characterized by the *partial correlation* between A and B given C , i.e. the correlation between residuals of linear regressions $C \rightarrow A$ and $C \rightarrow B$. One family of CI tests extends this insight to nonlinear generalizations of partial correlation, allowing the detection of nonlinear dependencies, as suggested by the general characterization of conditional independence of Daudin (1980). We consider specifically the Kernel-based Conditional Independence (KCI) (Zhang et al., 2011) statistic; and a successor, the Conditional Independence Regression CovariancE (CIRCE) (Pogodin et al., 2022), both described in Section 4. These methods replace the residuals of linear regression with a kernel analogue, derived from (infinite-dimensional) conditional feature means (Song et al., 2009; Grünewälder et al., 2012; Li et al., 2022b); they then use a kernel-based alternative to covariance (Gretton et al., 2005, 2007) to detect dependence between these residuals. Given the true conditional feature means and sufficient data for testing, these methods can detect general modes of conditional dependence, not just linear correlation.

Conditional feature mean estimation from data is not always a simple task, however: it is difficult in low-data regimes, and for some conditional dependencies it may even be impossible. In particular, nonparametric regression for conditional feature means suffers unavoidably from bias (Li et al., 2022b, 2024). This bias can easily create dependence between estimated residuals whose population counterparts are independent, inflating the rate of false positives above the design value for the test. Bias control is therefore essential in minimizing this effect, and controlling the rate of false positives.

We propose a set of techniques to mitigate this bias, bringing conditional independence tests closer to their nominal level. The key to our approach may be understood by comparing KCI with CIRCE, keeping in mind that both are zero only at conditional independence. The KCI is a covariance of residuals, and thus two regressions are needed in order to compute it (regression from C to A , and from C to B). CIRCE, by contrast, requires only regression from C to B , and computes the covariance of this residual with A alone. In other words, the second regression in KCI, from C to A , is not necessary for consistency of the test – both statistics are zero in population only at conditional independence. Where there is no true signal (at CI) and the regressions are independent, however, it is natural to expect that *residuals* from a regression to A may “appear less dependent” than A itself, debiasing the overall test (as formalized in Section 5). Thus, even imperfect $C \rightarrow A$ regression can reduce bias of the test statistic, and improve the Type I error (false detection rate), without compromising test consistency.

We introduce SplitKCI, a test statistic that (like KCI) uses both $C \rightarrow A$ and $C \rightarrow B$ regressions, but builds two independent estimators for one of the regressions. This reduces the effect of the bias from conditional mean estimation on the test statistic, leading to better Type I error control. To also achieve low Type II errors, we introduce a train/test data splitting heuristic that, in practice, improves the ability of the test to maintain its desired Type I error rate without sacrificing much in Type II error. Finally, we prove that the wild bootstrap technique for finding p -values for kernel-based test is applicable to KCI variance with empirical conditional mean estimates, improving over the commonly-used gamma approximation.

Testing terminology. The null hypothesis (denoted H_0) is $H_0: A \perp\!\!\!\perp B | C$, that A is independent of B given C . The alternative is $H_1: A \not\perp\!\!\!\perp B | C$. False positives (rejecting H_0

when it holds) are called Type I errors, and should be bounded by a fixed level α , e.g. 0.05. False negatives (failing to reject H_0 under H_1) are called Type II errors. Test power is the true positive rate, i.e. 1 minus the Type II error.

The rest of the paper is organised as follows. Section 2 discusses related work. Section 3 presents the concept of regression-based conditional independence tests. Section 4 introduces kernel methods, and in particular kernel methods-based tests. Section 5 presents SplitKCI, our approach to conditional independence testing, and discusses the motivation for changes w.r.t. the original KCI test. Section 6 discusses how to test for conditional independence with SplitKCI. Section 7 presents experiments on synthetic and real data. Section 8 concludes the paper with a discussion.

2 Related work

Uniformly valid conditional independence tests (with a correctly controlled false positive rate for any distribution) do not exist (Shah and Peters, 2020). Unlike for unconditional independence (Gretton et al., 2007; Albert et al., 2022), A and B may “seem” conditionally dependent until enough data is available to identify that C actually determines the dependence in a complex way; for instance, the construction of Shah and Peters (2020) essentially “hides” information on A in lower-order bits of C . Thus a test can never “commit” to conditional dependence (or to conditional independence), in contrast to unconditional settings where tests can successfully “commit” to dependence (rejecting the null). Thus, methods for CI testing must make (often implicit) assumptions on the underlying class of distributions: that is, they work only for a restricted set of nulls and alternatives.

A large body of work uses regression to estimate conditional dependence of A and B given C . This is achieved by building the test statistic from the respective residuals of $C \rightarrow A$ and $C \rightarrow B$ regressions. Several tests use finite-dimensional residuals, such as the Generalised Covariance Measure (GCM) (Shah and Peters, 2020), weighted GCM (Scheidegger et al., 2022), the Projected Covariance Measure (PCM) (Lundborg et al., 2022), and the Rao-Blackwellized Predictor Test (RBPT) (Polo et al., 2023). Kernel-based tests (Sun et al., 2007; Fukumizu et al., 2007; Strobl et al., 2019; Park and Muandet, 2020; Huang et al., 2022; Scetbon et al., 2022) instead rely on infinite-dimensional residuals (also see kernelized GCM, Fernández and Rivera, 2022). The latter can generally capture more complicated conditional dependencies, leading to better test power. As we will see below, however, they can struggle with correctly identifying conditional independence. In all cases, the type of regression used for each test is a practical choice; one common choice, including in this paper, is kernel ridge regression, due to its theoretical guarantees for conditional expectation estimation (Li et al., 2022b, 2024).

Another class of tests considers local permutations based on clusters of the conditioning variable C (Fukumizu et al., 2007; Sen et al., 2017; Neykov et al., 2021). This is done to simulate the null and compare it to the test data. However, test power in such approaches is sensitive to the marginal distribution of the conditioning variable C (Kim et al., 2022). These approaches can be thought of roughly as using a regression function from C to A and/or B that is piecewise-constant on these clusters in C .

CI tests are typically equipped with an approximate way to compute p-values based on the specific properties of each statistic. In situations where one can (approximately) sample

from either the $P(A|C)$ or the $P(B|C)$ distribution, several methods can guarantee level control by sampling from such distributions for any test statistic (e.g. CRT (Candes et al., 2018), CPT (Berrett et al., 2020); see for instance the conditional dependence coefficient of Azadkia and Chatterjee (2021) with a test based on CRT (Shi et al., 2024)). Given the ability to sample from these conditional distributions, one could also find an arbitrarily accurate regression; our aim is to improve the performance of tests for situations in which this sampling is not possible, due to a lack of data relative to the complexity of the conditional dependence.

3 Introduction to regression-based conditional independence testing

To define our conditional dependence measures, we will first need to characterize conditional independence. Based on the results of Daudin (1980), we will define conditional independence through conditional expectations. In practice, conditional expectation can be approximated with regression methods, giving rise to regression-based CI testing methods.

The definitions below are given for expectations of square-integrable test functions; considering the case where these functions are 0-1 indicators of events yields the more familiar version based on factoring probabilities.

Definition 1 (Daudin, 1980) *Random variables A and B are independent conditioned on C , denoted $A \perp\!\!\!\perp B|C$, if*

$$\mathbb{E}[g(A, C) h(B, C) | C] = \mathbb{E}[g(A, C) | C] \mathbb{E}[h(B, C) | C]$$

C -almost surely, for all square integrable functions $g \in L^2_{AC}$ and $h \in L^2_{BC}$.

Theorem 2 (Daudin, 1980) *Each of the following conditions hold if and only if $A \perp\!\!\!\perp B|C$,¹ where in each case the test functions h are in L^2_{BC} (i.e. $\mathbb{E}[h(B, C)^2] < \infty$), and the test functions g are in L^2_{AC} for (1) or L^2_A for (2) and (3).*

$$\mathbb{E}[g(A, C) h(B, C)] = 0 \quad \forall g, h \quad \text{s.t. } \mathbb{E}[g(A, C) | C] = 0 \text{ and } \mathbb{E}[h(B, C) | C] = 0; \quad (1)$$

$$\mathbb{E}[g(A) h(B, C)] = 0 \quad \forall g, h \quad \text{s.t. } \mathbb{E}[g(A) | C] = 0 \text{ and } \mathbb{E}[h(B, C) | C] = 0; \quad (2)$$

$$\mathbb{E}[g(A) h(B, C)] = 0 \quad \forall g, h \quad \text{s.t. } \mathbb{E}[h(B, C) | C] = 0. \quad (3)$$

In practice, Theorem 2 implies that we can select functions g and h and test whether they correlate in order to determine conditional dependence. More specifically, we can explicitly centre two L^2 functions (akin to Eq. (1)) and construct a test statistic on the basis of

$$\frac{1}{n} \sum_{i=1}^n [g(a_i, c_i) - \mathbb{E}[g(A, C) | C = c_i]] [h(b_i, c_i) - \mathbb{E}[h(B, C) | C = c_i]]. \quad (4)$$

Several tests follow this general approach: for instance, GCM (Shah and Peters, 2020) uses $g(A, C) = A, h(B, C) = B$. Weighted GCM (Scheidegger et al., 2022) and the Projected Covariance Measure (Lundborg et al., 2022) extend this to non-linear dependencies

1. The condition (2) is not explicitly stated by Daudin (1980), but follows from (3); see Pogodin et al. (2022), summarised in Section B.2.

for better test power. KCI (Zhang et al., 2011), the focus of our study, uses a different form of dependence, to be discussed shortly. For any choice of g and h , under conditional independence the statistic of (4) will straightforwardly converge to zero with increasing n . Absent conditional independence, however, the behaviour of (4) is determined by g and h . For instance, consider $A = C + \xi$, $B = C + \xi^2$ for a standard normal ξ . If g and h are linear, the test for conditional independence would amount to testing whether ξ and ξ^2 are correlated. As they are not, this test would fail to reject the null hypothesis of conditional independence. The kernel-based methods that we consider here address this issue by considering all possible g and h (in a dense subset of L^2), transforming the scalar-valued (4) into an infinite-dimensional vector.

The category of test statistics in (4) also requires us to compute the conditional expectation for the given functions. What happens if we estimate the conditional expectations incorrectly? In general, the test statistic might hallucinate dependence. Denote $\mu_{A|C} = \mathbb{E}[g(A, C) | C]$ and $\mu_{B|C} = \mathbb{E}[h(B, C) | C]$, and our estimates of these quantities $\hat{\mu}_{A|C}, \hat{\mu}_{B|C}$. Under conditional independence, our estimate of (4) becomes

$$\begin{aligned} & \frac{1}{n} \sum_i [g(a_i, c_i) - \hat{\mu}_{A|C}(c_i)] [h(b_i, c_i) - \hat{\mu}_{B|C}(c_i)] \\ &= \frac{1}{n} \sum_i [g(a_i, c_i) - \mu_{A|C}(c_i)] [h(b_i, c_i) - \mu_{B|C}(c_i)] \\ &+ \frac{1}{n} \sum_i [g(a_i, c_i) - \mu_{A|C}(c_i)] [\mu_{B|C}(c_i) - \hat{\mu}_{B|C}(c_i)] \\ &+ \frac{1}{n} \sum_i [\mu_{A|C}(c_i) - \hat{\mu}_{A|C}(c_i)] [h(b_i, c_i) - \mu_{B|C}(c_i)] \\ &+ \frac{1}{n} \sum_i [\mu_{A|C}(c_i) - \hat{\mu}_{A|C}(c_i)] [\mu_{B|C}(c_i) - \hat{\mu}_{B|C}(c_i)]. \end{aligned}$$

The first term on the right-hand side converges to zero as n grows, since $A \perp\!\!\!\perp B | C$. The remaining terms depend on the regression errors, however, and may not converge to zero with n ; the last term in particular may be large for “bad” g and h whose regression errors are correlated. This problem is exacerbated when looking for g and h with strong dependence under our estimated regressions, as do the kernel-based measures we discuss next.

If both of our conditional mean estimate remain imperfect as the number of test points $n \rightarrow \infty$, tests with sufficient power will always be able to detect this “spurious” dependence. In particular this implies that the higher the power of the conditional independence test, the more sensitive it will be to conditional mean estimation errors. One way to combat such behaviour is by computing the test statistic and the regressions on the same data points (as suggested for GCM by Shah and Peters 2020). We experimentally observe that this approach leads to inflated Type I errors for the kernel-based tests (although our method in Section 5.2 helps mitigate this; also see experiments in Section 7).

4 Kernel-based measures of conditional dependence

Kernel methods provide a way to construct infinite-dimensional g and h for (4) that, if the conditional means are estimated well, guarantee asymptotic power. A kernel $k : \mathcal{A} \times \mathcal{A} \rightarrow \mathbb{R}$ is a function such that $k(a, a') = \langle \phi(a), \phi(a') \rangle_{\mathcal{H}_a}$, where $\phi : \mathcal{A} \rightarrow \mathcal{H}_a$ is called a *feature map* and \mathcal{H}_a is a reproducing kernel Hilbert space (RKHS) of functions $f : \mathcal{A} \rightarrow \mathbb{R}$. The reproducing property of \mathcal{H}_a states that $\langle \phi(a), f \rangle_{\mathcal{H}_a} = f(a)$ for any $f \in \mathcal{H}_a$. For separable RKHSs \mathcal{H}_a and \mathcal{H}_b , we can define a space (see e.g. Gretton, 2013) of Hilbert-Schmidt operators $A, B : \mathcal{H}_a \rightarrow \mathcal{H}_b$, denoted $\text{HS}(\mathcal{H}_a, \mathcal{H}_b)$, with the inner product

$$\langle A, B \rangle_{\text{HS}(\mathcal{H}_a, \mathcal{H}_b)} = \sum_{i \in I, j \in J} \langle Ag_i, h_j \rangle_{\mathcal{H}_b} \langle Bg_i, h_j \rangle_{\mathcal{H}_b},$$

where $\{g_i\}_{i \in I}$ is any orthonormal basis of \mathcal{H}_a , and $\{h_j\}_{j \in J}$ is any orthonormal basis of \mathcal{H}_b .

For any $f_a \in \mathcal{H}_a$, $f_b \in \mathcal{H}_b$, the outer product $f_b \otimes f_a \in \text{HS}(\mathcal{H}_a, \mathcal{H}_b)$ is Hilbert-Schmidt; analogously to a Euclidean vector outer product, this outer product has that for $g_a \in \mathcal{H}_a$, $(f_b \otimes f_a)g_a = \langle f_a, g_a \rangle_{\mathcal{H}_a} f_b$ and $\langle A, f_b \otimes f_a \rangle_{\text{HS}} = \langle f_b, Af_a \rangle_{\mathcal{H}_b}$. We will often shorten $\text{HS}(\mathcal{H}_a, \mathcal{H}_b)$ to HS or HS_{ab} .

We can now define two conditional covariance operators (Fukumizu et al., 2004), based on the conditional mean embedding $\mu_{A|C}(C) = \mathbb{E}[\phi_a(A)|C]$. First, the Kernel-based Conditional Independence (KCI) operator, due to Zhang et al. (2011), is

$$\mathfrak{C}_{\text{KCI}} = \mathbb{E}[(\phi_a(A) - \mu_{A|C}(C)) \otimes \phi_c(C) \otimes (\phi_b(B) - \mu_{B|C}(C))]. \quad (5)$$

This is a *covariance operator* because, for any $g \in \mathcal{H}_a$ and $h \in \mathcal{H}_{bc}$ (a space of functions on $\mathcal{B} \times \mathcal{C}$),

$$\langle g, \mathfrak{C}_{\text{KCI}} h \rangle = \mathbb{E}[(g(A) - \mathbb{E}[g(A)|C])(h(B, C) - \mathbb{E}[h(B, C)|C])].$$

Thus, if (and only if) $\mathfrak{C}_{\text{KCI}} = 0$, a version of (2) where we additionally restrict $g \in \mathcal{H}_a$, $h \in \mathcal{H}_{bc}$ holds. Note that the original definition used $\phi_{bc}(B, C) - \mu_{BC|C}(C)$; if $\phi_{bc}(B, C) = \phi_b(B) \otimes \phi_c(C)$ as in radial basis kernels, the definition here (adapted from Pogodin et al. (2022)) is the same but avoids estimation of $\mu_{C|C}(C) = \phi_c(C)$, which is problematic as discussed in Section B.2. The original paper also swapped the roles of A and B .

Although Theorem 2 uses L^2 functions, we can define analogous RKHS statistics using an *L^2 -universal* kernel, one whose RKHS is dense in L^2 ; common choices such as the Gaussian kernel $k(a, a') = \exp(-\|a - a'\|^2/(2\sigma^2))$ are L^2 -universal (Fukumizu et al., 2007; Sriperumbudur et al., 2011). By continuity, if no RKHS functions have nonzero conditional covariance, then the same applies to L^2 functions, and so $\mathfrak{C}_{\text{KCI}} = 0$ iff $A \perp\!\!\!\perp B | C$.² To test for conditional independence, we can therefore use the squared HS norm of the covariance operator as the test statistic, since under the null,

$$H_0 : \|\mathfrak{C}_{\text{KCI}}\|_{\text{HS}}^2 = 0.$$

2. The proof for KCI and KCI-like statistics can be straightforwardly adapted from Th. 2.5 in (Pogodin et al., 2022). L^2 -universality of the kernel is sufficient, but probably not necessary; it is not necessary for unconditional dependence (Gretton, 2015; Szabó and Sriperumbudur, 2018).

Using the CI condition in (3), Pogodin et al. (2022) introduced the Conditional Independence Regression Covariance (CIRCE) operator to avoid centring A in cases where $\phi_a(A)$ is changing, e.g. because $\phi_a(A)$ incorporates learned neural net features as a part of the mapping:

$$\mathfrak{C}_{\text{CIRCE}} = \mathbb{E}[\phi_a(A) \otimes \phi_c(C) \otimes (\phi_b(B) - \mu_{B|C}(C))]. \quad (6)$$

4.1 Conditional mean embeddings via kernel ridge regression

The main challenge of using KCI is in estimating the conditional mean embeddings (CME) $\mu_{A|C}$ and/or $\mu_{B|C}$ from data. The standard way to estimate CMEs is through kernel ridge regression (KRR) (Song et al., 2009; Grünwald et al., 2012). Using m points, $\lambda > 0$ as the ridge regression parameter, and with some abuse of notation denoting Φ_C to be an operator from \mathbb{R}^m to \mathcal{H}_c such that $\Phi_C h = \sum_{i=1}^m h_i \phi(c_i)$ and analogously for Φ_A , the KRR estimate of the CME is

$$\hat{\mu}_{A|C} = \Phi_C(K_C + \lambda m I_m)^{-1} \Phi_A. \quad (7)$$

At any point c , the CME is therefore estimated as

$$\hat{\mu}_{A|C}(c) = K_{cC}(K_C + \lambda m I_m)^{-1} \Phi_A, \quad (8)$$

where the m -dimensional vector K_{cC} is evaluated as $(K_{cC})_i = k_c(c, c_i)$.

Performance of KRR for this task is well-studied, making it a useful tool for theoretical analysis of tests that rely on conditional means. As shown by Li et al. (2022b), Th. 2, for RKHS-valued g and h , KRR converges as $O(m^{-\frac{\beta-\gamma}{2(\beta+p)}})$ (which is shown to be minimax optimal). Informally speaking, $\beta \in [1, 2]$ and $p > 0$ determine the smoothness of the conditional mean operators, and γ determines the norm in which we consider KRR convergence. For the L^2 norm, applicable to finite-dimensional g and h , we have $\gamma = 0$ and thus the best-case convergence rate can be arbitrarily close to $O(m^{-1/2})$. For RKHS-valued g and h , however, we need to consider RKHS norm convergence corresponding to $\gamma = 1$. As a result, the best-case convergence rate is (arbitrarily close to) $O(m^{-1/4})$. In both cases, $p \rightarrow \infty$ makes convergence arbitrarily slow.

5 SplitKCI

As discussed above, CME estimation in an RKHS with m data points typically converges as $O(m^{-1/4})$ or slower. In contrast, for a fixed CME, the estimate of the KCI statistic converges as $O(n^{-1/2})$ (Pogodin et al., 2022, Cor. C.6). In this section, we show that CME estimation errors appear as (spurious) dependence in the test statistic. This is an issue: for large enough n (e.g. if $n = m$ when using the same data for both CME estimation and testing), the $O(m^{-1/4})$ noise bias in the test statistic would be significantly larger than the $O(n^{-1/2})$ variation expected under the null. Thus, this test would frequently reject the null simply due to CME estimation errors and not true conditional dependence, failing to have any level control.

A straightforward solution to this problem is to ensure that $n \ll m$. This, however, directly reduces the power of the test to detect true conditional dependencies, as well as spurious ones. We present two approaches to mitigate this problem that when combined, achieve both level control (low Type I error) and high power (low Type II error). In

Section 5.1, we present SplitKCI and demonstrate that it significantly reduces the effect of CME estimation bias on the KCI statistic. In Section 5.2, we present a heuristic for choosing the train/test split, i.e. m and n , to achieve high power without sacrificing level control.

5.1 Reducing CME estimation bias in KCI

We start by analysing the effect of an incorrect CME, which introduces an additional bias into our dependence measure even at population level, $n = \infty$. We refer to the n points used for statistic evaluation as $\mathcal{D}_{\text{test}}^n$, the m_{bc} points used for estimating $\mu_{B|C}$ as $\mathcal{D}_{\text{train}}^{m_{bc}}$, and the m_{ac} points used for estimating $\mu_{A|C}$ as $\mathcal{D}_{\text{train}}^{m_{ac}}$. For our theoretical analysis, we assume that the test data is independent of the training data.

We first define a generic KCI-type operator: for $\beta : \mathcal{C} \rightarrow \mathcal{H}_a$ and $\tau : \mathcal{C} \rightarrow \mathcal{H}_b$,

$$\mathfrak{C}(\beta, \tau) = \mathbb{E}[(\phi_a(A) - \beta(C)) \otimes \phi_c(C) \otimes (\phi_b(B) - \tau(C))] . \quad (9)$$

Then $\mathfrak{C}_{\text{KCI}} = \mathfrak{C}(\mu_{A|C}, \mu_{B|C})$ and $\mathfrak{C}_{\text{CIRCE}} = \mathfrak{C}(0, \mu_{B|C})$. In practice, however, we only have access to operators based on CME estimates $\hat{\mu}_{A|C}(c) = \mu_{A|C}(c) + \hat{b}_{A|C}(c)$ and an analogous $\hat{\mu}_{B|C}$. Thus, for given CME estimators, the underlying operators we estimate in a test are

$$\hat{\mathfrak{C}}_{\text{KCI}} = \mathfrak{C}\left(\mu_{A|C} + \hat{b}_{A|C}, \mu_{B|C} + \hat{b}_{B|C}\right), \quad \hat{\mathfrak{C}}_{\text{CIRCE}} = \mathfrak{C}\left(0, \mu_{B|C} + \hat{b}_{B|C}\right) .$$

Under H_0 , we have that $\mathfrak{C}_{\text{KCI}} = \mathfrak{C}(\mu_{A|C}, \mu_{B|C}) = 0$, and therefore

$$\hat{\mathfrak{C}}_{\text{KCI}} = \mathbb{E}\left[\hat{b}_{A|C} \otimes \phi_c(C) \otimes \hat{b}_{B|C}\right] ,$$

leading to a test statistic that might deviate from zero:

$$\|\hat{\mathfrak{C}}_{\text{KCI}}\|_{\text{HS}}^2 = \mathbb{E}\left(\left\langle \hat{b}_{A|C}(C), \hat{b}_{A|C}(C') \right\rangle_{\mathcal{H}_a} k_c(C, C') \left\langle \hat{b}_{B|C}(C), \hat{b}_{B|C}(C') \right\rangle_{\mathcal{H}_b}\right) , \quad (10)$$

where C, C' are independent copies.

Thus, if the bias is ignored, the statistic will appear to indicate dependence, even though none exists—potentially leading to excessive Type I error rates. For CIRCE, the $\langle \hat{b}_{A|C}(C), \hat{b}_{A|C}(C') \rangle_{\mathcal{H}_a}$ term in the last equation is replaced by $\langle \mu_{A|C}(C), \mu_{A|C}(C') \rangle_{\mathcal{H}_a}$, yielding a potentially larger term when the regression bias is small. We can view the larger bias of CIRCE through the lens of double robustness (Chernozhukov et al., 2018) of KCI: since conditional dependence is measured in terms of a product of the residuals, KCI only needs to get both regressions somewhat right, while CIRCE needs the second regression to be very accurate to reduce bias.

To mitigate the bias in KCI estimation, we first show that various KCI-like estimates of conditional independence asymptotically behave the same way:

Theorem 3 *For functions $\beta^{(1)}, \beta^{(2)} : \mathcal{C} \rightarrow \mathcal{H}_a$ and $\tau^{(1)}, \tau^{(2)} : \mathcal{C} \rightarrow \mathcal{H}_b$ bounded uniformly in RKHS norm across train set sizes, define the test statistic T as a Hilbert-Schmidt inner product*

$$T(\beta^{(1)}, \tau^{(1)}, \beta^{(2)}, \tau^{(2)}) = \left\langle \mathfrak{C}(\beta^{(1)}, \tau^{(1)}), \mathfrak{C}(\beta^{(2)}, \tau^{(2)}) \right\rangle_{\text{HS}}.$$

Under H_0 , $T \rightarrow 0$ if any one of $\beta^{(1)}, \tau^{(1)}, \beta^{(2)}, \tau^{(2)}$ converges to the corresponding $\mu_{A|C}$ or $\mu_{B|C}$ in RKHS norm.

Under H_1 , $T \rightarrow t > 0$ if either both $\beta^{(1)}, \beta^{(2)} \rightarrow \mu_{A|C}$ or both $\tau^{(1)}, \tau^{(2)} \rightarrow \mu_{B|C}$ in RKHS norm.

The proof, in Section A.1, shows equivalence between this measure and KCI/CIRCE. The empirical estimator of T over n points follows the standard (quadratic-time) HSIC estimator (with $O(n^{-1/2})$ convergence; see, e.g., Pogodin et al., 2022, Corollary C.6):

$$T_n = \frac{1}{n^2} \mathbf{1}_n^\top ((HK_A^\star H) \odot K_C \odot K_B^\star) \mathbf{1}_n, \quad (11)$$

where $A \odot B$ is the elementwise product, $H = I_n - \frac{1}{n} \mathbf{1}_n \mathbf{1}_n^\top$ is the ‘‘centering matrix’’, and $(K_C)_{ij} = k_c(c_i, c_j)$. In general, K_A^\star (and, analogously, K_B^\star) is defined as

$$(K_A^\star)_{ij} = \left\langle \phi_a(a_i) - \beta^{(1)}(c_i), \phi_a(a_j) - \beta^{(2)}(c_j) \right\rangle. \quad (12)$$

For KCI, all parts of the test statistic use CME estimates, i.e. $\beta^{(1)} = \beta^{(2)} = \hat{\mu}_{A|C}$ and $\tau^{(1)} = \tau^{(2)} = \hat{\mu}_{B|C}$. For CIRCE, $\beta^{(1)} = \beta^{(2)} = 0$ and therefore $(K_A)_{ij} = k_a(a_i, a_j)$.

Furthermore, to work with symmetric matrices, in experiments we will symmetrize the measure as $\frac{1}{2}(T(\beta^{(1)}, \tau^{(1)}, \beta^{(2)}, \tau^{(2)}) + T(\beta^{(2)}, \tau^{(2)}, \beta^{(1)}, \tau^{(1)}))$.

As a consequence of Theorem 3, we can choose how to estimate CME for each part of $T(\dots)$ to minimize the bias term under the null (Eq. (10)). For that, we define SplitKCI:

Definition 4 (SplitKCI) For CME estimates $\hat{\mu}_{A|C}^{(1)}, \hat{\mu}_{A|C}^{(2)}$ trained over equal non-overlapping splits of a dataset, and analogously for $\hat{\mu}_{B|C}$, we define SplitKCI as

$$\text{SplitKCI} = T \left(\hat{\mu}_{A|C}^{(1)}, \hat{\mu}_{B|C}^{(1)}, \hat{\mu}_{A|C}^{(2)}, \hat{\mu}_{B|C}^{(2)} \right) \quad (13)$$

Eq. (13) satisfies the conditions of Theorem 3, meaning it asymptotically characterises conditional independence.

To analyse SplitKCI, we make standard assumptions to guarantee the CME estimator’s convergence. For a space of real-valued Lebesgue square integral (with respect to measure π) functions $L_2(\pi)$ and an embedding $I_\pi : \mathcal{H}_a \rightarrow L_2(\pi)$ that maps $f \in \mathcal{H}_a$ to its π -equivalence class $[f]$, we can define interpolation spaces and the corresponding norm as follows:

Definition 5 (β -interpolation space, Steinwart and Scovel, 2012; Li et al., 2022b) For $\beta \geq 0$, a countable index set I , a non-increasing sequence $(\mu_i)_{i \in I} > 0$, and a family $(e_i)_{i \in I} \in \mathcal{H}_a$, such that $([e_i])_{i \in I}$ is an orthonormal basis (ONB) of $\overline{\text{ran } I_\pi} \subseteq L_2(\pi)$ and $(\mu_i^{1/2} e_i)_{i \in I}$ is an ONB of $(\ker I_\pi)^\perp \subseteq \mathcal{H}_a$, the β -interpolation space is defined as

$$[\mathcal{H}]_a^\beta = \left\{ \sum_{i \in I} a_i \mu_i^{\beta/2} [e_i] : (a_i)_{i \in I} \in \ell_2(I) \right\} \in L_2(\pi).$$

It is equipped with the β -power norm

$$\left\| \sum_{i \in I} a_i \mu_i^{\beta/2} [e_i] \right\|_{\beta} = \|(a_i)_{i \in I}\|_{\ell_2(I)} = \left(\sum_{i \in I} a_i^2 \right)^{1/2}.$$

In particular for $\beta = 0$ we have $\|\cdot\|_0 = \|\cdot\|_{L_2(\pi)}$, and for $\beta = 1$ we go back to the standard RKHS norm, i.e. $\|[f]\|_1 = \|f\|_{\mathcal{H}_a}$ for $f \in \mathcal{H}_a$ (and $[f] = I_{\pi}(f) \in L_2(\pi)$). For $\beta > 1$, we get a subspace of the original space with smoother operators.

For Hilbert-Schmidt spaces $\text{HS}(\mathcal{H}_a, \mathcal{H}_b)$, we can similarly define vector-valued interpolation spaces $[\text{HS}]^{\beta}$ (and the corresponding norm) by defining a mapping to $L_2(\pi, \mathcal{H}_b)$. See Def. 3 of Li et al. (2022b) for the full definition.

Assumption 1 (CME rates, Fischer and Steinwart, 2020) (EVD) *The eigenvalues μ_i of $C_{CC} = \mathbb{E}[\phi_c(C) \otimes \phi_c(C)]$ decay as $\mu_i \leq c_{\mu} i^{-1/p}$, for some $c_{\mu} > 0$ and $p \in (0, 1]$. (Boundedness) $k_c(C, C') \leq 1$.³ (SRC) The conditional mean operators satisfy $\mu_{A|C} \in [\text{HS}_{ac}]^{\beta}, \mu_{B|C} \in [\text{HS}_{bc}]^{\beta}$ for the same $\beta \in [1, 2]$.⁴*

We use the same β for both operators only for simplicity; all proofs generalize to different interpolation space parameters β_{ac}, β_{bc} .

Theorem 6 (Bias in KCI and SplitKCI) *Under Assumption 1 and using independent data splits $\mathcal{D}_{\text{train}}^{m_{ac}}$ (for KCI), $\mathcal{D}_{\text{train}}^{\frac{m_{ac}}{2}(1)}, \mathcal{D}_{\text{train}}^{\frac{m_{ac}}{2}(2)}$ (for SplitKCI), and analogously (and independently) for the $C \rightarrow B$ regression, the biases defined as the expectation over both the train and test data $b = \mathbb{E} T(\dots)$ under H_0 are bounded as*

$$b_{\text{KCI}} \leq ((1+K_1) \|\mu_{A|C}\|_{\beta}^2 + K_2) ((1+K_1) \|\mu_{B|C}\|_{\beta}^2 + K_2) m_{ac}^{-\frac{\beta-1}{\beta+p}} m_{bc}^{-\frac{\beta-1}{\beta+p}},$$

$$b_{\text{SplitKCI}} \leq 4 \|\mu_{A|C}\|_{\beta}^2 \|\mu_{B|C}\|_{\beta}^2 m_{ac}^{-\frac{\beta-1}{\beta+p}} m_{bc}^{-\frac{\beta-1}{\beta+p}}.$$

for $K_1, K_2, K_3 > 0$ (independent of m_{ac}, m_{bc}).

Proof [Proof idea] The proof, in Section A.2, compares the bias terms using the CME estimator rates due to (Li et al., 2022b). The KCI bound is much larger due to the constants in the upper bounds of the CME estimator – realistically, these constants are unlikely to be tight. The b_{KCI} bound is a sum of two terms (with a common multiplier): $\|\mu_{A|C}\|_{\beta}^2$, coming from the bias due to non-zero ridge parameter λ , and a (much larger due to large K_1) term $K_1 \|\mu_{A|C}\|_{\beta}^2 + K_2$, which comes from $\langle \hat{\mu}_{A|C}(c_i), \hat{\mu}_{A|C}(c_j) \rangle$. For SplitKCI, the latter term is zero, as we use two independent CME estimators in $\langle \hat{\mu}_{A|C}^{(1)}(c_i), \hat{\mu}_{A|C}^{(1)}(c_j) \rangle$; the former one is doubled since each regression uses $\frac{m_{ac}}{2}$ points and $2^{\frac{\beta-1}{\beta+p}} < 2$. \blacksquare

3. This satisfies the EMB condition of Fischer and Steinwart (2020), with $\alpha = 1$ and $A = 1$.

4. While $\beta > 2$ is possible, convergence doesn't improve due to the saturation effect for ridge regression (Li et al., 2022a).

This change is somewhat counter-intuitive: finding the CME is hard, so we want to use as much data as we can. But due to the slow scaling with m_{ac} , halving the data doesn't hurt the overall estimate as much as decorrelating the errors improves it. Even for SplitKCI, however, the remaining bias term is still large unless m_{ac} and m_{bc} are large. This approach is similar to double cross-fitting of estimators for GCM-like measures (McClean et al., 2024), although in our case we have to use independent datasets for estimating the same regression twice (as opposed to fitting $C \rightarrow A$ and $C \rightarrow B$ regressions on independent datasets).

5.2 A heuristic for choosing train/test split ratio for SplitKCI

So far the discussion on de-biasing of KCI has not included the crucial point we made in the introduction: for kernel-based methods, CME estimation convergence much slower than the test statistic itself: in the best case for CME, only $O(n^{-1/4})$ convergence is possible (Li et al., 2022b) (and worst-case convergence can be arbitrarily slow), as opposed to $O(n^{-1/2})$ convergence of HSIC-based statistics for a given CME (Gretton et al., 2007).

Thus, if we use the same number of data points for both CME estimation and evaluation of the test statistic, we might obtain a test statistic that treats errors in the CME estimate as a significant correlation of residuals, leading to rejection of the null. In addition, using the training points (or a subset of those) for testing can introduce unexpected correlations into the test statistic (we discuss this in Section C.3.1). Therefore, we need to balance the number of train (for CME) and test (for the test itself) data points.

To the best of our knowledge, previous literature on KCI-based tests either did not use a train/test split at all, or used manually selected splits, which is impractical given that splitting influences both Type I and II errors.

One way to overcome the slow convergence rates of CME estimators is to use auxiliary data to estimate one regression, e.g. $\mu_{B|C}$, very well. In some cases, such as genetic studies (Candes et al., 2018), auxiliary (B, C) data is available. Another option is to use the same data as both the train and test sets, as done in other tests, since the in-sample, i.e. train, regression errors are smaller than out-of-sample. This is the approach taken for GCM (see the discussion preceding Th. 8 of Shah and Peters 2020 and further discussed by Lundborg et al. 2022) and the original KCI paper (Zhang et al., 2011). However, since CME estimation convergence is much slower for kernel-based tests than for tests with finite-dimensional CMEs, like GCM, in-sample regression errors can still be too large to achieve level control; this is confirmed in experiments below.

Therefore, we require a way to choose train and test data splits. We outline two requirements for the train/test split procedure. For Type I error control, at least one CME estimator, $\hat{\mu}_{A|C}$ or $\hat{\mu}_{B|C}$, should be able to show independence from C for a chosen number of test points. For maximizing test power, we need to use as many test points as possible (while preserving the first quality).

To address the first point, we first note that for the true CME $\mu_{A|C}$, the $\phi_a(A) - \mu_{A|C}(C)$ residuals should be independent of C :

$$\mathfrak{C}_{\text{train/test split}}^{AC} = \mathbb{E} [(\phi_a(A) - \mu_{A|C}(C)) \otimes \phi_c(C)] = 0.$$

For a given train/test split, we can evaluate $\|\hat{\mathfrak{C}}_{\text{train/test split}}^{AC}\|^2$ (with or without train splitting into two regressions) and then compute the p -value for $H_0 : \|\mathfrak{C}_{\text{train/test split}}^{AC}\|^2 = 0$.

We use this idea to build a heuristic for evaluating a given train/test split ratio. While this is a heuristic, we extensively evaluate it on several tasks in Section 7. To choose the train/test split, we

1. compute $\|\mathfrak{C}_{\text{train/test split}}^{AC}\|^2$ and $\|\mathfrak{C}_{\text{train/test split}}^{BC}\|^2$;
2. compute p -values p_A and p_B from wild bootstrap (see Section 6.1);
3. repeating this r times, estimate the rejection rate $\omega = \frac{1}{r} \sum_i \mathbb{I}[p_A^i \leq \alpha] \mathbb{I}[p_B^i \leq \alpha]$.

If ω is larger than the level α , we conclude that the CME estimates are not accurate enough to detect conditional independence. Then, we change the split ratio to use fewer test points and repeat the procedure. The exact algorithm used in the experiments is summarized in Algorithm 3 (in Section B.2).

6 Statistical testing with SplitKCI

To use KCI-like measures for statistical testing, we need to compute (approximate) p -values for the data. This is not straightforward: under the null, and assuming perfect estimates of $\mu_{A|C}$ and $\mu_{B|C}$, these statistics are distributed as an infinite weighted sum of chi-squared variables (Zhang et al., 2011; Fernández and Rivera, 2022), rather than the Gaussian that is often the case with other statistics. Moreover, the parameters of this mixture depend on the data distribution and the kernels, and so has to be approximated. The original KCI paper used a moment-matched Gamma approximation (Zhang et al., 2011), which lacks formal guarantees. In our preliminary experiments, this approximation tended to not produce correct p -values (Fig. 10 in Section B.2), so we turn to the wild bootstrap approximation (Wu, 1986; Shao, 2010; Fromont et al., 2012; Leucht and Neumann, 2013; Chwialkowski et al., 2014).

6.1 Wild bootstrap for computing p -values

Following Chwialkowski et al. (2014), we provide wild bootstrap guarantees for an uncentered V-statistic version \widehat{V} of (11) (as well as analogous versions for CIRCE and SplitKCI), defined as

$$\widehat{V} = \frac{1}{n^2} \mathbf{1}_n^\top \left[(qq^\top) \odot \widehat{K}_A^c \odot K_C \odot \widehat{K}_B^c \right] \mathbf{1}_n, \quad (14)$$

where $q = \mathbf{1}_n$ is a vector of all ones. We are justified in removing the centring from Eq. (11) because the estimator is asymptotically centred on the training data. If q is instead a vector of Rademacher variables (± 1 with equal probability), we refer to the wild bootstrap quantity (14) as \widehat{V}^* .

The following theorem guarantees the validity of the wild bootstrap for KCI, CIRCE, and SplitKCI, taking into account the estimation error of the CME. To the best of our knowledge, this result is novel, including for the KCI.

Theorem 7 (Wild bootstrap) *Assume that m_{ac} and m_{bc} dominate $n^{\frac{\beta+p}{\beta-1}}$ asymptotically for β and p as in Assumption 1, and that k_a , k_b and k_c are bounded by 1. (i) Under the null, $n\widehat{V}^*$ and $n\widehat{V}$ converge weakly to the same distribution. (ii) Under the alternative, \widehat{V}^* converges to zero in probability, and \widehat{V} converges to a positive constant.*

The proof (in Section A.3) generalizes the techniques developed by Chwialkowski et al. (2014) for HSIC to KCI, CIRCE, and SplitKCI, but takes into account imperfect CME estimates.

Theorem 7 shows (pointwise) asymptotic validity of the wild bootstrap, taking into account the estimation error of the CME. Theorem 7(i) shows that the test is asymptotically *well-calibrated*: the Type I error is asymptotically controlled at the desired level. That $n\hat{V}^*$ converges to the right distribution for a single data sample follows analogously to Theorem 3.1 of Leucht and Neumann (2013); see also their Algorithm. Theorem 7(ii) shows that the test is *consistent*: the Type II error of any alternative tends to zero asymptotically.

6.2 Full test for SplitKCI

The full testing procedure using SplitKCI remains similar to KCI: for a chosen set of kernels over A, B, C , we first compute CME estimates, then compute CME-centred estimates of the kernel matrices, and finally construct the test statistic and find the approximate p-value of this static. Unlike for KCI, we use the train/test split heuristic of Section 5.2 to compute CME estimates over the train set and kernel matrices over the test set; for a given training set, we compute two CME estimates using equal parts of the training set (the ‘‘Split’’ in SplitKCI) to reduce estimation bias in KCI; finally, we compute p-values using wild bootstrap (Section 6.1). The full test procedure is summarized in Algorithm 1. Note that the estimator (11) can be replaced with an unbiased estimate (21), which we found gives a slight improvement. For SplitKCI_A only, $\hat{\mu}_{B|C}$ is computed using the full train set $\mathcal{D}_{\text{train}}^m$.

Data: $\mathcal{D} = \{(a_i, b_i, c_i)\}_{i=1}^N$	
Train/test splits: $\mathcal{D}_{\text{train}}^m, \mathcal{D}_{\text{test}}^n$	# Algorithm 3
Train splits: $\mathcal{D}_{\text{train}}^m = \mathcal{D}_{\text{train}}^{\frac{m}{2}(1)} \cup \mathcal{D}_{\text{train}}^{\frac{m}{2}(2)}$	# Theorem 4
Train set: CME estimation	# Algorithm 2
$\hat{\mu}_{A C}^{(1)}, \hat{\mu}_{B C}^{(1)}$ using $\mathcal{D}_{\text{train}}^{\frac{m}{2}(1)}$, $\hat{\mu}_{A C}^{(2)}, \hat{\mu}_{B C}^{(2)}$ using $\mathcal{D}_{\text{train}}^{\frac{m}{2}(2)}$	
Test set: statistic evaluation	
K_A^c, K_C, K_B^c using $\mathcal{D}_{\text{test}}^n$	# Eq. (12)
$\text{SplitKCI} = \frac{1}{n^2} \mathbf{1}_n^\top ((HK_A^c H) \odot K_C \odot K_B^c) \mathbf{1}_n$	# Eq. (11)
Result: SplitKCI p-value with wild bootstrap	
$\hat{V}_k^* = \frac{1}{n^2} \mathbf{1}_n^\top [(q q^\top) \odot \hat{K}_A^c \odot K_C \odot \hat{K}_B^c] \mathbf{1}_n$ for $(q_k)_i = \pm 1$	# Eq. (14)
$p = \frac{1}{K+1} (1 + \sum_{k=1}^K \mathbb{I}[\text{SplitKCI} \leq \hat{V}_k^*])$	
Algorithm 1: SplitKCI test.	

7 Experiments

We perform an extensive analysis of SplitKCI and competing tests in several tasks and testing scenarios. We use two synthetic and one real datasets of various complexity and dimensionality, described in Section 7.1. For the first low-dimensional synthetic dataset, we analyse the train/test splitting heuristic (introduced Section 7.4) in Section 7.2, and then evaluate all methods on the task in Section 7.3. We repeat the analysis of the heuristic on high-dimensional synthetic neural data in Section 7.4, and in Sections 7.5 and 7.6 compare the methods’ performance with different amounts of available data. We conclude the exper-

imental section with analysis of real insurance data in Section 7.7. Code for all experiments is available at github.com/romanpogodin/kernel-ci-testing.

7.1 Description of tasks and the experimental setup

Synthetic data from a post-nonlinear model First, we evaluate the methods on data from a post-nonlinear model (Zhang and Hyvärinen, 2012), in particular a variation of the model used in the original KCI paper (Zhang et al., 2011). This model generates A and B as nonlinear random (but fixed for each trial) noisy functions of C . While A and B are one-dimensional, C can be high-dimensional, allowing to assess robustness of testing methods to dimensionality of C .

We generate the data for a d -dimensional $C \sim \mathcal{N}(0, 1/d)$ as follows:

$$A = G_a \left(\frac{1}{d+1} \left(E_a + \sum_{i=1}^d F_{a,i}(C_i + \xi_{a,i}) \right) \right),$$

$$B = G_b \left(\frac{1}{d+1} \left(E_b + \sum_{i=1}^d F_{b,i}(C_i + \xi_{b,i}) \right) \right),$$

where $E_a, E_b \sim \mathcal{N}(0, 1)$, all G and F are random functions (sampled as random convex combinations of $f_1(x) = x$, $f_2(x) = \tanh(x)$, and $f_3(x) = \tanh(x^3)$).

We use $\xi_{a,i}$ and $\xi_{b,i}$ to “hide” conditional dependence in the first coordinate. In all cases, $\xi_{a,i} = \xi_{b,i} = 0$ for $i > 1$. Under H_0 , $\xi_{a,0}, \xi_{b,0} \sim \mathcal{N}(0, 1)$ (independently). Under H_1 , $\xi_{a,0} = \xi_{b,0} \sim \mathcal{N}(0, 1)$. Thus, as dimensionality of the problem increases, it becomes progressively harder to detect conditional dependence.

Synthetic neural data We evaluate the tests on high-dimensional synthetic data that mimics neural recordings. We use the RatInABox toolbox (George et al., 2024), which models behavior and neural activity of a rat freely running in a generated 2d environment. RatInABox can model several types of neurons observed experimentally; we use the head direction and conjunctive cell models (see Section C for the exact model) as they generate non-trivial dependencies in the data. As A , we use head direction cells: each has a preferred orientation of the rat’s head, and is only active around those orientations (Knierim et al., 1995). As B , we use conjunctive cells: each has a preferred head direction similar to A , but is only active in certain locations in the environment (Sargolini et al., 2006), which can be obtain as a combination of position-only grid cells and head direction cells. For both cell types, their activity can be well explained by the animal’s head direction and position, which we use as the conditioning variable C . This setup is similar to the RatInABox conjunctive cells demo, and is visualised in Fig. 1.

We test the following question: is head direction selectivity of conjunctive cells B driven by the head direction cells A ? In other words, under the null the head direction and the conjunctive cells are independent given the actual head direction (and other behavioural variables like position that might contribute to the noise of both populations). Under the alternative, the head direction cells modulate activity of position-selective cells, giving rise to conjunctive cells.

We use 100 cells for A and B , and a 4-dimensional C (head direction vector and position). To generate the data, we simulate the animal’s behaviour for several minutes, and then

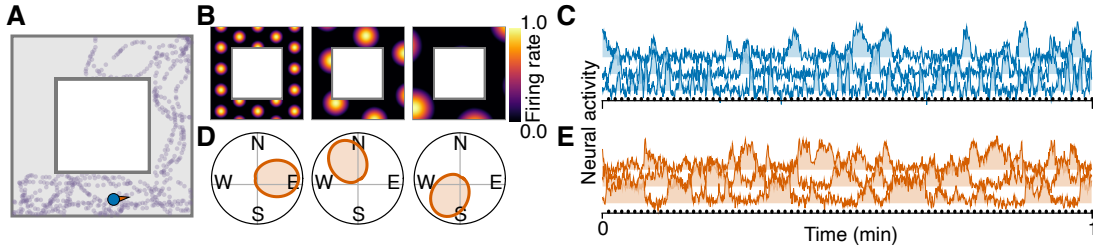


Figure 1: RatInABox data visualisation. **A.** Simulated rat trajectory in a square box with a blocked off centre. **B.** Activation patterns of three grid cells w.r.t. rat’s position in the box. **C.** Simulated neural activity of the cells in **B**. Black dots indicate which data points are used in the dataset. **D.** Activation patterns of three head direction cells w.r.t. rat’s head direction (polar coordinates). **E.** Same as **C**, but for the head direction cells.

subsample the activity to obtain approximately i.i.d. data (choosing the sampling rate based on the noise autocorrelation). Other experimental details are postponed to Section C.

Car insurance data Following the experiments of Polo et al. (2023), we test our methods on the car insurance dataset originally collected from four US states and multiple insurance companies by Angwin et al. (2017).⁵

The dataset has three variables: car insurance price A , minority neighborhood indicator B (defined as more than 66% non-white in California and Texas, and more than 50% in Missouri and Illinois), and driver’s risk C (with additional equalization of driver-related variables; see Angwin et al. 2017).

Alternative tests We compare kernel-based methods to GCM (Shah and Peters, 2020) and RBPT2 (Polo et al., 2023). Both are regression-based methods, so we use the same set of kernels over C as for KCI variants, and do not require knowledge of $P(B | C)$. GCM looks at correlations between $\mathbb{E}[A | C]$ and $\mathbb{E}[B | C]$ (estimated through kernel ridge regression, but with finite-dimensional outputs). RBPT2 compares how well A can be predicted by $g(B, C) = \mathbb{E}[A | B, C]$ vs. $h = \mathbb{E}[g(B, C) | C]$, also relying on kernel ridge regressions. We describe these methods in detail in Section B.4. For RBPT2, we found the original method to be heavily biased against rejection of the null; we found an analytical correction and called the method RBPT2’ (see Section B.4). Finally, we don’t show CIRCE performance as it significantly underperforms vanilla KCI (see Fig. 10 in Section C).

Data regimes We evaluate all tests in two different data regimes. *Standard*: (A, B, C) points available in triplets. *Auxiliary data*: (A, B, C) points along with an independent set of (B, C) points. In both regimes, we need the data to first estimate $\hat{\mu}_{A|C}$ and $\hat{\mu}_{B|C}$, and then to evaluate the test statistic.

7.2 Influence of train/test splitting on KCI-style methods for a post-nonlinear model

First, we evaluate the train/test splitting heuristic introduced in Section 5.2 on the post-nonlinear model (see Section 7.1). For $\alpha = 0.05$ (for both test level and split threshold), we

5. Data available from <https://projects.propublica.org/graphics/carinsurance>.

evaluate KCI and SplitKCI (Algorithm 1) for test to train ratios between 0.1 and 0.8, and datast sizes $N = 200$ and $N = 400$.

For both choices of N , Type I error is similar between SplitKCI and KCI (Fig. 2A, top). In contrast, the split rejection rate (Fig. 2A, bottom) for SplitKCI reflects its Type I error much better than for KCI, as indicated by slower raise of the split rejection rate for higher test/train ratios.

Type II error is similar between SplitKCI and KCI across all split ratios. However, the split rejection rate again better reflects the changes in Type II error for SplitKCI. Therefore, SplitKCI with the train/test splitting heuristic can choose split ratios that favour smaller Type II errors (also indicated by asterisks in Fig. 2B placed roughly where the split reject rate crosses the $\alpha = 0.05$ threshold).

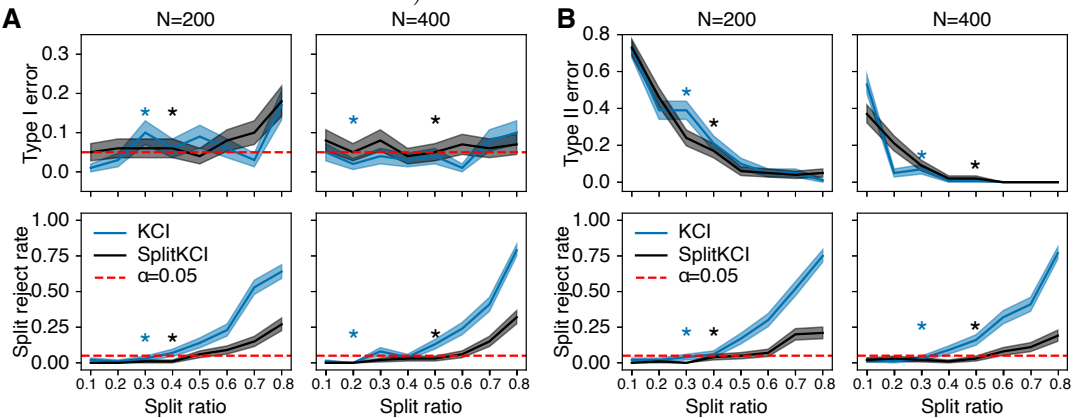


Figure 2: Train/test splitting in a post-nonlinear model with $d = 4$ and a fixed dataset size $N = n + m$ (for n test and m training points). **A.** Type I error (top) vs. rejection rate for the train/test split heuristic (bottom) for different dataset sizes N and test to train split ratios. **B.** Type II error (top) vs. rejection rate for the train/test split heuristic (bottom) for different dataset sizes N and split ratios. Lines/shaded area: mean/ \pm SE over 100 trials, $\alpha = 0.05$. Asterisks: approximate split ratios from Algorithm 3 to show performance of the splitting heuristic.

7.3 Methods comparison for a post-nonlinear model

Next, we evaluate performance over varying number of data points $N = n + m$. For SplitKCI, we find the train/test split ratio using Algorithm 3 for one random seed, and then evaluate the rest of the random seeds on the chosen split ratio. For KCI and RBPT2', we show results for $n = 100$ test points. For GCM, we don't use splitting, as was recommended by the original paper (Shah and Peters, 2020).

Under H_0 and across all dimensionalities and total number for data points, all methods generally hold level (Fig. 3A), although RBPT' and KCI are above level for some dimensionalities. As we determine the train/test split for SplitKCI using the proposed heuristic, this result shows that the heuristic can correctly find the ratio sufficient for the required Type I error.

Under H_1 , for $N = 200$ (Fig. 3B, left) KCI and SplitKCI show worse Type II error than the other two methods, although notably SplitKCI performs comparably to KCI. For

$N = 400$, SplitKCI performs significantly better than KCI and on par with the other two methods (Fig. 3B, right). First, this means that $N = 400$ provides enough data for KCI-style methods to detect conditional dependence in this task. Second, this results shows that the train/test splitting heuristic is powerful enough to make use of the additional data, while the standard KCI with a fixed split is not.

In this task, not using a train/test split at all was a valid strategy not only for GCM, but also for KCI/SplitKCI (see Fig. 12 in the Appendix): just like GCM, KCI/SplitKCI hold level and achieve nearly zero Type II error. However, as we will see in the next section, this strategy only works for simple tasks.

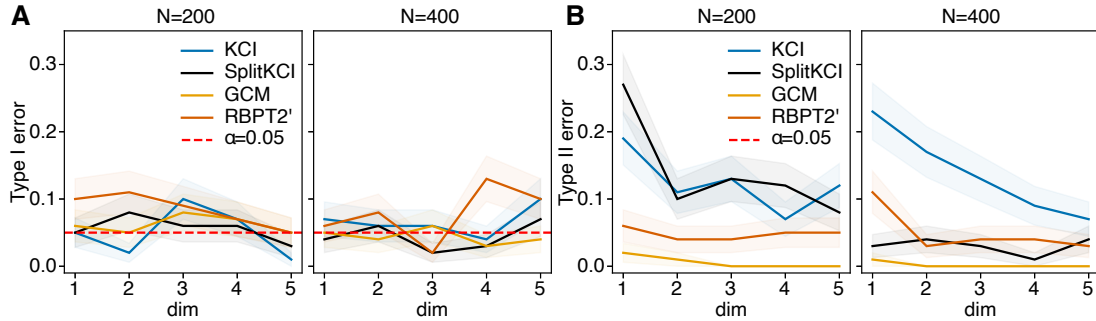


Figure 3: Post-nonlinear model experiments for increasing dimensionality of the task and a fixed dataset size $N = n + m$ (for n test and m training points). **A.** Type I error for $N = 200$ (left) and $N = 400$ (right) data points. **B.** Type II error for $N = 200$ (left) and $N = 400$ (right) data points. Lines/shaded area: mean/ \pm SE over 100 trials, $\alpha = 0.05$.

7.4 Influence of train/test splitting on KCI-style methods for synthetic neural data

For the synthetic neural data, we again first we evaluate the train/test splitting heuristic introduced in Section 5.2. For $\alpha = 0.05$ (for both test level and split threshold), we evaluate KCI and SplitKCI for test to train ratios between 0.1 and 0.8, for three dataset sizes (200, 500, 1000).

For all budget sizes, SplitKCI shows Type I error dynamics which is significantly better than for regular KCI (Fig. 4, top). For KCI, the split rejection rate (Fig. 4, bottom, blue lines) steadily increases with split size, meaning that it cannot serve as a reliable measure of Type I error. In contrast, for SplitKCI with 500 and 1000 data points (Fig. 4, bottom, black lines), the split rejection rate can reliably select split ratios that result in Type I error control.

For Type II error control, both methods show similar trends (Fig. 5): SplitKCI can reliably select split ratios that result in small Type II error, while KCI cannot (which is also indicated by asterisks in Fig. 5 placed roughly where the split reject rate crosses the $\alpha = 0.05$ threshold).

These results show interplay of several factors that affect SplitKCI performance. Compared to KCI, CME estimation bias has less effect on SplitKCI, leading to lower Type I errors. For the same reason, the proposed heuristic for choosing the train/test split ratio better reflects Type I performance. Finally, lower bias allows to use more test points, which in turn leads to lower Type II errors as the test becomes more sensitive to true conditional

dependence. More generally, these results confirm our discussion in Section 5 about the effect of the number of train points m and test points n : larger n/m always leads to higher Type I errors.

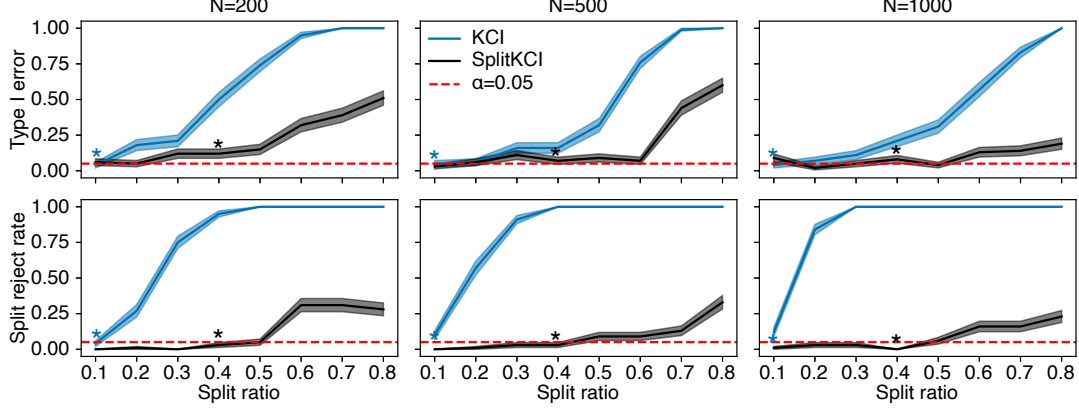


Figure 4: Train/test splitting in the synthetic neural data. Type I error (top) vs. rejection rate for the train/test split heuristic (bottom) for different dataset sizes $N = n + m$ and test to train (n/m) split ratios. Lines/shaded area: mean/ \pm SE over 100 trials, $\alpha = 0.05$. Asterisks: approximate split ratios from Algorithm 3 to show performance of the splitting heuristic.

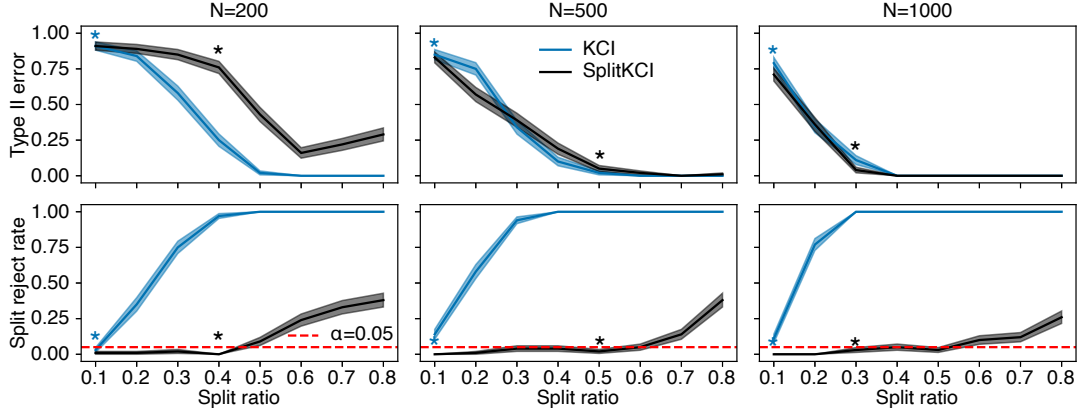


Figure 5: Train/test splitting in the synthetic neural data. Type II error (top) vs. rejection rate for the train/test split heuristic (bottom) for different dataset sizes $N = n + m$ and test to train (n/m) split ratios. Lines/shaded area: mean/ \pm SE over 100 trials, $\alpha = 0.05$. Asterisks: approximate split ratios from Algorithm 3 to show performance of the splitting heuristic.

7.5 SplitKCI holds level and achieves high power for synthetic neural data

Here, we evaluate performance over varying number of data points $N = n+m$. For SplitKCI, we find the train/test split ratio using Algorithm 3 for one random seed, and then evaluate the rest of the random seeds on the chosen split ratio. For KCI and RBPT2', we show results for $n = 100$ test points. For GCM, we don't use splitting, as was recommended by

the original paper (Shah and Peters, 2020). Other fixed splitting strategies for all methods perform as well or worse (see Figs. 14 and 15).

Type I error Under the null, SplitKCI achieved level control, as well as GCM and (for larger N) RBPT2' (Fig. 6A). KCI struggled much more, especially at smaller dataset sizes. This illustrates that the automated splitting procedure for SplitKCI allows the test to hold level without pre-determined train/test splits (as well as for fixed splits, see Fig. 14).

Type II error Under the alternative, all methods apart from KCI quickly achieved low error (Fig. 6B). As we used a fixed size of the test dataset for KCI, increasing the total budget N led to increasingly better CME estimates. Therefore, for larger N , KCI estimate becomes less biased, which in turns leads to less frequent rejection. If we increase the number of test points, the power would increase as well (as shown in Fig. 5). However, KCI in this case would fail to hold level. In contrast, our train/test approach for SplitKCI allows to find splits that achieve high power while still holding level, even though the optimal split size varies across N (see Fig. 14 for $n = 100$ and $n = m$ performance).

Using the train/test splitting for KCI and SplitKCI was crucial for Type I performance, as hinted earlier in Section 3. While GCM and many other tests often don't use a train/test split (with GCM achieving the best results in that setting in all of our experiments), KCI and SplitKCI without a train/test split do not achieve level α in this task (see Section C.3.1).

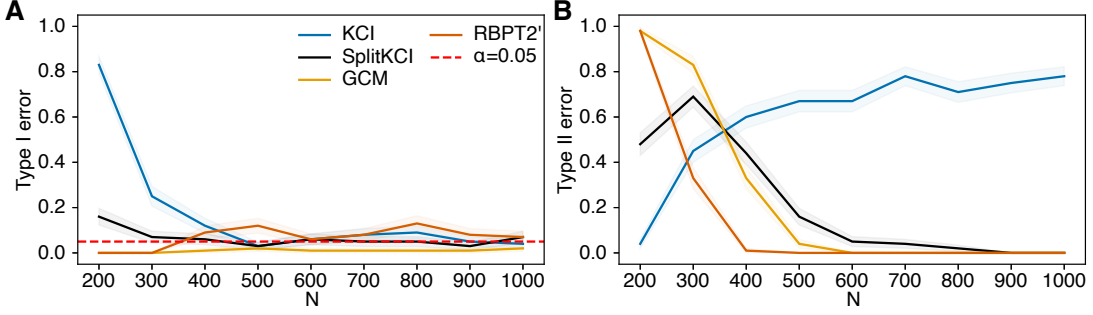


Figure 6: Synthetic neural data experiments for an increasing dataset size $N = n + m$ (for n test and m training points). **A.** Type I error. **B.** Type II error. Lines/shaded area: mean/ \pm SE over 100 trials, $\alpha = 0.05$.

7.6 SplitKCI holds level and achieve high power with auxiliary data for synthetic neural data

In some application, such as genetic studies (Candes et al., 2018), full triplets of (A, B, C) points could be scarcely available, while (B, C) auxiliary is not (e.g. because it is easier to collect). For the synthetic neural data, one could imagine that simultaneous recordings from two neural populations A and B are expensive, while collecting just one population B along with behavioural data C is cheaper. As CME estimation bias for both KCI and SplitKCI depend on the size of the (B, C) multiplicatively (see Theorem 6), we expect all tests to perform better in this regime.

We studied the setting in which the number of (A, B, C) points is fixed and small (we use $N = 200$ and $N = 400$ points), but we have access to an independent large set of $M = (B, C)$ points. We therefore use N for the $C \rightarrow A$ regressions and testing, and M

points for the $C \rightarrow B$ regressions. We don't use a train/test split over N for KCI, SplitKCI, and GCM, and use $n = 100$ for RBPT'.

Type I error Under the null, all methods apart from RBPT2' held level without train/test splitting over (A, B, C) (Fig. 7A,C; for RBPT2', a better Type I error was achieved for 100/100 train/test split). For SplitKCI, splitting did not affect Type I error much, but KCI was at level only without train/test splitting (see Figs. 16 and 17). A potential explanation is that due to small m , the $C \rightarrow A$ tends to overfit, producing small in-sample and large out-of-sample errors. (The effect on SplitKCI is smaller since the train data is split, and so half of the residuals for each regression are always out-of-sample.)

Type II error Under the alternative, for $N = 200$ all methods generally showed poor Type II error (Fig. 7B), with GCM having no power. For RBPT2', its better performance is consistent with poor Type I error control. For $N = 400$ (Fig. 7D), Type II error decreases for all methods, staying the lowest for RBPT' and SplitKCI, and the highest for GCM and KCI.

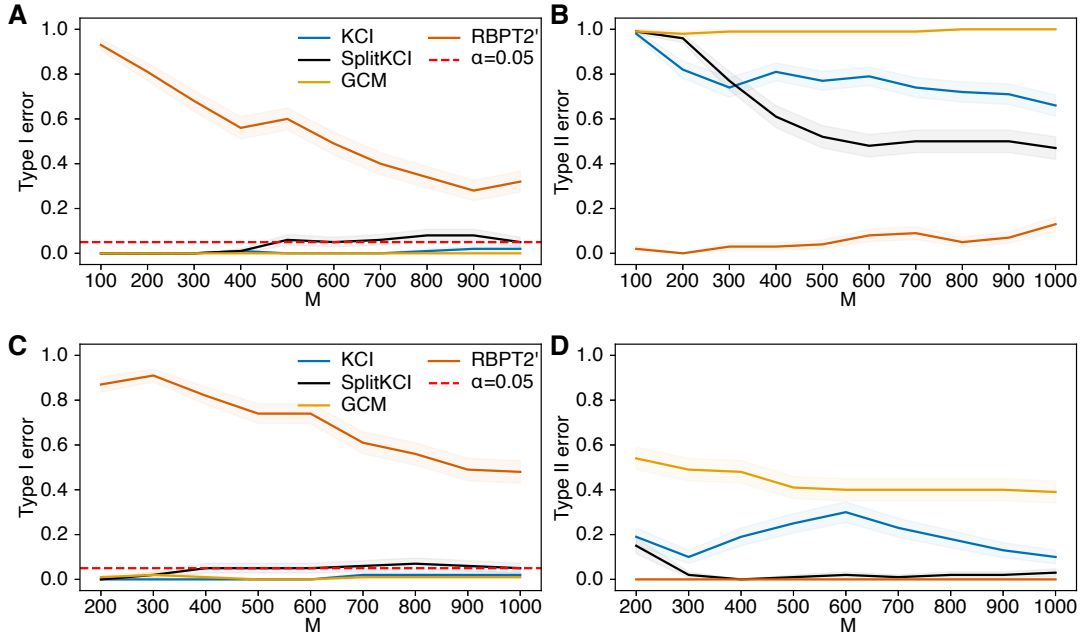


Figure 7: Synthetic neural data experiments for a fixed (A, B, C) dataset size (N points), but increasing amount of auxiliary (B, C) data (M points). **A.** Type I error for 200 (A, B, C) points. **B.** Type II error. **C-D.** Same as **A-B**, but for 400 (A, B, C) points. Lines/shaded area: mean/ \pm SE over 100 trials, $\alpha = 0.05$.

7.7 Car insurance data

We follow the data assessment experiment from Polo et al. (2023) to evaluate different methods under a *simulated* H_0 . Polo et al. (2023) divided the driver's risk into 20 clusters, and shuffled the corresponding insurance price (per company and per state; about 1-2k

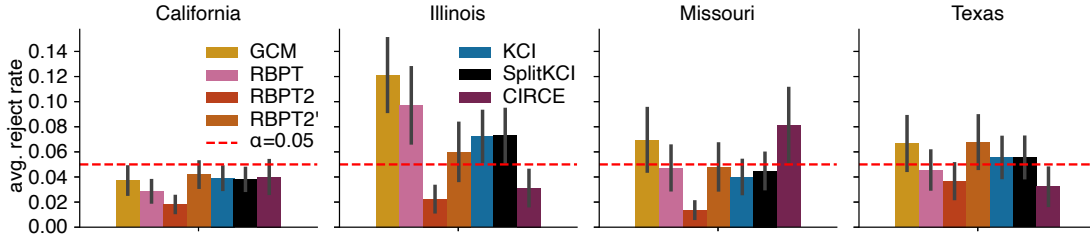


Figure 8: Simulated null hypothesis for the car insurance data. For each state, the average rejection rate across several companies is calculated as in Polo et al. (2023). Mean \pm SE over 50 trials.

points for each, which is enough to avoid merging train and test data). The resulting data was evaluated for several tests, with average (over companies) rejection rate reported as Type I error. We find (see Fig. 8) that both KCI and SplitKCI produce robust results at the desired $\alpha = 0.05$ level. As well, RBPT2 with or without bias correction holds level. In contrast, GCM, RBPT and CIRCE in some cases produce larger Type I errors.

Finally, evaluated all methods on the full dataset to test for conditional independence. Using a 70/30% train/test split as in Polo et al. (2023) (with 24-34k points total per state), we computed p -values for each method. As in Polo et al. (2023), RBPT and RBPT2 did not reject the null at $\alpha = 0.05$ for California data, but did for the other states. All other methods, including the bias-corrected RBPT2', rejected the null for all states. The results are summarized in Fig. 9, suggesting that most methods, apart from RBPT and RBPT2, reject the null at $\alpha = 0.05$ for all states. CIRCE (not shown in the main text) performed similar to KCI/SplitKCI but produced less accurate Type 1 errors.

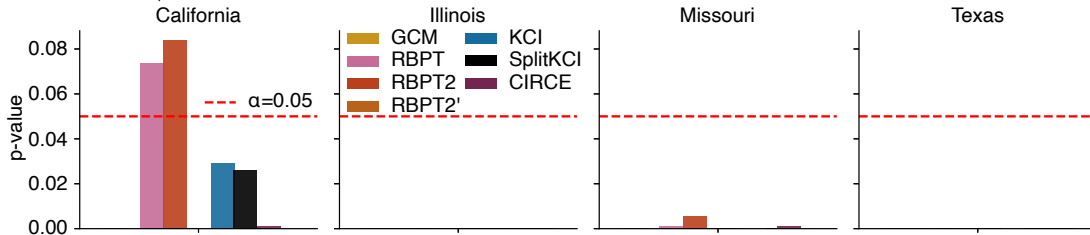


Figure 9: Evaluation of all methods on the full car insurance dataset (without averaging over companies, unlike in the simulated null in Fig. 8). Expanded from Polo et al. (2023) by adding KCI-based methods.

8 Discussion

We introduced SplitKCI, a version of the KCI (Zhang et al., 2011) test that is less biased towards rejection and can be combined with a train/test data splitting heuristic to achieve Type I error control under the null and also Type II error minimisation under the alternative. We also showed that the wild bootstrap approach for producing p -values for kernel-based independence tests can be generalised to KCI and SplitKCI with imperfect CME estimates. In experiments, we showed that SplitKCI can indeed hold level and produce lower Type II errors than KCI, and also than non-kernel based methods.

Several extensions of our work are possible. Other kernel-based measures of conditional dependence (Fukumizu et al., 2007; Strobl et al., 2019; Park and Muandet, 2020; Scetbon et al., 2022) also rely on CME and are limited by CME estimator’s quality; our insights might be used to improve alternative methods.

As CME estimation accuracy is crucial for test performance, parametric alternatives to kernel ridge regression might provide better estimates in some cases. For instance, when A is categorical, we can replace kernel ridge regression with logistic regression, or any classifier, with a linear kernel on top; this can produce accurate predictions of A that are not limited by simple hand-crafted kernels. It might also be possible to estimate $\mu_{A|C}$ with parametric methods e.g. as $\hat{\mu}_{A|C}(c) = f_\theta(c)\Phi_a$ – cf. (8) – similar to regression-based methods like GCM (Shah and Peters, 2020).

Next, our wild bootstrap result shows pointwise asymptotic level control. While it might be possible to show uniformly asymptotic level control for distributions satisfying our assumptions, we believe this is more challenging for kernel-based measures than for settings with asymptotically normal statistics (e.g. GCM). One approach could be to find an asymptotically normal (Split)KCI estimator, as in the cross-HSIC statistic for unconditional independence testing (Shekhar et al., 2023), but it is unclear how this drastically different approach would perform in practice.

Using a kernel-based wild bootstrap can lead to non-asymptotic Type I error guarantees in certain testing scenarios, such as MMD two-sample tests (Schrab et al., 2023, 2022b; Fromont et al., 2012) and HSIC independence tests (Albert et al., 2022). In other cases, the control is only asymptotic, as in KSD goodness-of-fit (Schrab et al., 2022a; Key et al., 2021). It might be possible to develop non-asymptotic results for KCI-style tests as well. Shah and Peters (2020) proved that if a conditional independence test always controls the Type I error non-asymptotically, then it cannot have power against *any* alternative. Throughout this paper, however, we assume that we can reliably estimate the conditional means – that is, the underlying operators are smooth enough. This restricts the space of nulls and alternatives for which kernel-based methods work, suggesting that it might be possible to develop results similar to non-asymptotically valid tests that can achieve minimax-optimal power (Schrab et al., 2023; Biggs et al., 2023; Kim and Schrab, 2023).

Conditional dependence tests are often used for sensitive domains in which the conclusions of a study can have significant societal impacts (e.g. Angwin et al., 2017). A further important topic for future work is therefore test interpretability, since conditional (in)dependence may be caused by unknown confounding variables.

Acknowledgments and Disclosure of Funding

This work was supported by the Natural Sciences and Engineering Research Council of Canada (NSERC Discovery Grant: RGPIN-2020-05105; Discovery Accelerator Supplement: RGPAS-2020-00031; Arthur B. McDonald Fellowship: 566355-2022), the Canada CIFAR AI Chairs program, a CIFAR Learning in Machine and Brains Fellowship, U.K. Research and Innovation (grant EP/S021566/1), and the Gatsby Charitable Foundation. This research was enabled in part by support provided by Calcul Québec and the Digital Research Alliance

of Canada. The authors acknowledge the material support of NVIDIA in the form of computational resources.

The authors would like to thank Namrata Deka and Liyuan Xu for helpful discussions.

We present the proofs of the technical results in Section A. Details about other measures of conditional independence are presented in Section B. Section C contains experimental details, as well as additional experiments.

Appendix A. Proofs

A.1 SplitKCI definition

Theorem 3 *For functions $\beta^{(1)}, \beta^{(2)} : \mathcal{C} \rightarrow \mathcal{H}_a$ and $\tau^{(1)}, \tau^{(2)} : \mathcal{C} \rightarrow \mathcal{H}_b$ bounded uniformly in RKHS norm across train set sizes, define the test statistic T as a Hilbert-Schmidt inner product*

$$T(\beta^{(1)}, \tau^{(1)}, \beta^{(2)}, \tau^{(2)}) = \left\langle \mathfrak{C}(\beta^{(1)}, \tau^{(1)}), \mathfrak{C}(\beta^{(2)}, \tau^{(2)}) \right\rangle_{\text{HS}}.$$

Under H_0 , $T \rightarrow 0$ if any one of $\beta^{(1)}, \tau^{(1)}, \beta^{(2)}, \tau^{(2)}$ converges to the corresponding $\mu_{A|C}$ or $\mu_{B|C}$ in RKHS norm.

Under H_1 , $T \rightarrow t > 0$ if either both $\beta^{(1)}, \beta^{(2)} \rightarrow \mu_{A|C}$ or both $\tau^{(1)}, \tau^{(2)} \rightarrow \mu_{B|C}$ in RKHS norm.

Proof Under H_0 , assuming w.l.o.g. that $\beta^{(1)} \rightarrow \mu_{A|C}$ in RKHS norm and using the fact that other CME estimates are bounded,

$$\begin{aligned} T(\beta^{(1)}, \tau^{(1)}, \beta^{(2)}, \tau^{(2)}) &\rightarrow T(\mu_{A|C}, \tau^{(1)}, \beta^{(2)}, \tau^{(2)}) \\ &= \left\langle \mathfrak{C}(\mu_{A|C}, \tau^{(1)}), \mathfrak{C}(\beta^{(2)}, \tau^{(2)}) \right\rangle. \end{aligned}$$

Using linearity of expectation, we have that

$$\begin{aligned} \mathfrak{C}(\mu_{A|C}, \tau^{(1)}) &= \mathbb{E} \left((\phi_a(A) - \mu_{A|C}(C)) \otimes \phi_c(C) \otimes (\phi_b(B) - \tau^{(1)}(C)) \right) \\ &= \mathbb{E} \left((\phi_a(A) - \mu_{A|C}(C)) \otimes \phi_c(C) \otimes \phi_b(B) \right) = \mathfrak{C}(\mu_{A|C}, 0) =_{H_0} 0, \end{aligned}$$

and therefore $T =_{H_0} 0$.

Under H_1 , again assuming w.l.o.g. that $\tau^{(1)}, \tau^{(2)} \rightarrow \mu_{B|C}$ in RKHS norm and using the fact that other CME estimates are bounded,

$$\begin{aligned} T(\beta^{(1)}, \tau^{(1)}, \beta^{(2)}, \tau^{(2)}) &\rightarrow T(\beta^{(1)}, \mu_{B|C}, \beta^{(2)}, \mu_{B|C}) \\ &= \left\langle \mathfrak{C}(\beta^{(1)}, \mu_{B|C}), \mathfrak{C}(\beta^{(2)}, \mu_{B|C}) \right\rangle \\ &= \left\langle \mathfrak{C}(0, \mu_{B|C}), \mathfrak{C}(0, \mu_{B|C}) \right\rangle = \|\mathfrak{C}_{\text{CIRCE}}\|_{\text{HS}}^2 >_{H_1} 0. \end{aligned}$$

■

A.2 Bias

Theorem 6 (Bias in KCI and SplitKCI) *Under Assumption 1 and using independent data splits $\mathcal{D}_{\text{train}}^{m_{ac}}$ (for KCI), $\mathcal{D}_{\text{train}}^{\frac{m_{ac}}{2}(1)}, \mathcal{D}_{\text{train}}^{\frac{m_{ac}}{2}(2)}$ (for SplitKCI), and analogously (and independently) for the $C \rightarrow B$ regression, the biases defined as the expectation over both the*

train and test data $b = \mathbb{E} T(\dots)$ under H_0 are bounded as

$$b_{\text{KCI}} \leq ((1+K_1) \|\mu_{A|C}\|_\beta^2 + K_2) ((1+K_1) \|\mu_{B|C}\|_\beta^2 + K_2) m_{ac}^{-\frac{\beta-1}{\beta+p}} m_{bc}^{-\frac{\beta-1}{\beta+p}},$$

$$b_{\text{SplitKCI}} \leq 4 \|\mu_{A|C}\|_\beta^2 \|\mu_{B|C}\|_\beta^2 m_{ac}^{-\frac{\beta-1}{\beta+p}} m_{bc}^{-\frac{\beta-1}{\beta+p}}.$$

for $K_1, K_2, K_3 > 0$ (independent of m_{ac}, m_{bc}).

Proof First, we will consider the most generic case of SplitKCI, later assuming that $\widehat{\mu}_{A|C}^{(1)} = \widehat{\mu}_{A|C}^{(2)}$ and $\widehat{\mu}_{B|C}^{(1)} = \widehat{\mu}_{B|C}^{(2)}$ for KCI. Denoting

$$(\widehat{K}_A^c)_{ij} = \frac{1}{2}(\widehat{K}_A^{12})_{ij} + \frac{1}{2}(\widehat{K}_A^{21})_{ij}, \quad (\widehat{K}_A^{12})_{ij} = \langle \phi_a(a_i) - \widehat{\mu}_{A|C}^{(1)}(c_i), \phi_a(a_j) - \widehat{\mu}_{A|C}^{(2)}(c_j) \rangle,$$

and similarly $(\widehat{K}_B^c)_{ij}$ computed over for test points i, j . Additionally decomposing all CME estimates as

$$(\widehat{K}_{BC|C})_{ij} = (K_C \odot \widehat{K}_B^c)_{ij} = k_c(c_i, c_j) \langle \phi_b(b_i) - \widehat{\mu}_{B|C}(c_i), \phi_b(b_j) - \widehat{\mu}_{B|C}(c_j) \rangle,$$

where we decompose the empirical estimate of the mean into the true one, the distance between the true one and the expected estimate given the ridge parameters, and finally between the ridge mean and its estimate (so that the last term is zero-mean).

Under the null, we can immediately remove the terms with the true centered variables $\phi_a(a_i) - \mu_{A|C}^{(1)}(c_i)$:

$$\begin{aligned} & \mathbb{E} (\widehat{K}_A^{12})_{ij} (K_C)_{ij} (\widehat{K}_B^{12})_{ij} \\ &= \mathbb{E} \langle \phi_a(a_i) - \widehat{\mu}_{A|C}^{(1)}(c_i), \phi_a(a_j) - \widehat{\mu}_{A|C}^{(2)}(c_j) \rangle (K_C)_{ij} (\widehat{K}_B^{12})_{ij} \\ &=_{H_0} \mathbb{E} \langle \delta\mu_{A|C}^\lambda(c_i) + \delta\widehat{\mu}_{A|C}^{(1)\lambda}(c_i), \delta\mu_{A|C}^\lambda(c_j) + \delta\widehat{\mu}_{A|C}^{(2)\lambda}(c_j) \rangle (K_C)_{ij} (\widehat{K}_B^{12})_{ij} \\ &= \mathbb{E} [\langle \delta\mu_{A|C}^\lambda(c_i), \delta\mu_{A|C}^\lambda(c_j) \rangle + \langle \delta\widehat{\mu}_{A|C}^{(1)\lambda}(c_i), \delta\widehat{\mu}_{A|C}^{(2)\lambda}(c_j) \rangle] (K_C)_{ij} (\widehat{K}_B^{12})_{ij} \\ &=_{H_0} \mathbb{E} [\langle \delta\mu_{A|C}^\lambda(c_i), \delta\mu_{A|C}^\lambda(c_j) \rangle + \langle \delta\widehat{\mu}_{A|C}^{(1)\lambda}(c_i), \delta\widehat{\mu}_{A|C}^{(2)\lambda}(c_j) \rangle] k_c(c_i, c_j) \langle \delta\widehat{\mu}_{B|C}(c_i), \delta\widehat{\mu}_{B|C}(c_j) \rangle, \end{aligned}$$

where in the third line we took the expectation over $\mathcal{D}_{\text{train}}^{\frac{m_{ac}}{2}(1)}, \mathcal{D}_{\text{train}}^{\frac{m_{ac}}{2}(2)}$ using the facts that $\mathbb{E} \delta\widehat{\mu}_{A|C}^{1/2\lambda} = 0$ and that all data splits (apart from $\mathcal{D}_{\text{train}}^{\frac{m_{ac}}{2}(1)}, \mathcal{D}_{\text{train}}^{\frac{m_{ac}}{2}(2)}$) are independent. Repeating the same calculation for $(\widehat{K}_B^{12})_{ij}$,

$$\begin{aligned} & \mathbb{E} (\widehat{K}_A^{12})_{ij} (K_C)_{ij} (\widehat{K}_B^{12})_{ij} \\ &= \mathbb{E} \left([\langle \delta\mu_{A|C}^\lambda(c_i), \delta\mu_{A|C}^\lambda(c_j) \rangle + \langle \delta\widehat{\mu}_{A|C}^{(1)\lambda}(c_i), \delta\widehat{\mu}_{A|C}^{(2)\lambda}(c_j) \rangle] k_c(c_i, c_j) \right. \\ & \quad \left. [\langle \delta\mu_{B|C}^\lambda(c_i), \delta\mu_{B|C}^\lambda(c_j) \rangle + \langle \delta\widehat{\mu}_{B|C}^{(1)\lambda}(c_i), \delta\widehat{\mu}_{B|C}^{(2)\lambda}(c_j) \rangle] \right). \end{aligned}$$

For SplitKCI we can take the expectation w.r.t. the train data, removing the zero-mean $\langle \delta\widehat{\mu}_{A|C}^{(1)\lambda}(c_i), \delta\widehat{\mu}_{A|C}^{(2)\lambda}(c_j) \rangle$ term. Therefore, if we take expectations over the test points i, j

under H_0 ,

$$\begin{aligned} b_{\text{KCI}} &= \mathbb{E} \left(\left[\left\langle \delta\mu_{A|C}^\lambda(c_i), \delta\mu_{A|C}^\lambda(c_j) \right\rangle + \left\langle \delta\hat{\mu}_{A|C}^\lambda(c_i), \delta\hat{\mu}_{A|C}^\lambda(c_j) \right\rangle \right] k_c(c_i, c_j) \right. \\ &\quad \left. \left[\left\langle \delta\mu_{B|C}^\lambda(c_i), \delta\mu_{B|C}^\lambda(c_j) \right\rangle + \left\langle \delta\hat{\mu}_{B|C}^\lambda(c_i), \delta\hat{\mu}_{B|C}^\lambda(c_j) \right\rangle \right] \right), \\ b_{\text{SplitKCI}} &= \mathbb{E} \left(\left[\left\langle \delta\mu_{A|C}^\lambda(c_i), \delta\mu_{A|C}^\lambda(c_j) \right\rangle \right] k_c(c_i, c_j) \right. \\ &\quad \left. \left[\left\langle \delta\mu_{B|C}^\lambda(c_i), \delta\mu_{B|C}^\lambda(c_j) \right\rangle \right] \right). \end{aligned}$$

Now, for datasets of equal size, the KCI bias is clearly larger than both SplitKCI ones. However, in practice we would use twice as many points for KCI, so the exact scaling of the terms is important.

To bound the individual terms, we first note that since we assumed the CME is well-specified, we can use the reproducing property $\langle \mu_{A|C}(c), h \rangle_{\mathcal{H}_a} = \langle \mu_{A|C}, \phi_c(c) \otimes h \rangle_{\text{HS}}$ to show that $\|\mu_{A|C}(c)\| \leq \|\mu_{A|C}\| k_c(c, c)^{1/2}$, and hence by Cauchy-Schwarz

$$\left\langle \delta\mu_{A|C}^\lambda(c_i), \delta\mu_{A|C}^\lambda(c_j) \right\rangle \leq \|\delta\mu_{A|C}^\lambda\|^2 k_c(c_i, c_i)^{1/2} k_c(c_j, c_j)^{1/2} \leq \|\delta\mu_{A|C}^\lambda\|^2,$$

assuming the kernels are bounded by 1. We can extend this to all products, again using independence of data splits (so $\|\delta\hat{\mu}_{A|C}^\lambda\|^2$ and $\|\delta\hat{\mu}_{B|C}^\lambda\|^2$ are independent) and the fact that $\|\delta\mu_{A|C}^\lambda\|^2$ and $\|\delta\mu_{B|C}^\lambda\|^2$ are deterministic,

$$\begin{aligned} b_{\text{KCI}} &\leq_{H_0} \left[\|\delta\mu_{A|C}^\lambda\|^2 + \mathbb{E} \|\delta\hat{\mu}_{A|C}^\lambda\|^2 \right] \left[\|\delta\mu_{B|C}^\lambda\|^2 + \mathbb{E} \|\delta\hat{\mu}_{B|C}^\lambda\|^2 \right], \\ b_{\text{SplitKCI}} &\leq_{H_0} \left[\|\delta\mu_{A|C}^\lambda\|^2 \right] \left[\|\delta\mu_{B|C}^\lambda\|^2 \right]. \end{aligned}$$

Now, with our assumptions about CME convergence, we can directly use Theorem 2 of Li et al. (2022b), (with $\gamma = 1$, $\alpha = 1$ and $\beta \in (1, 2]$ to match the required HS norm and the well-specified case): $\|\delta\hat{\mu}_{B|C}^\lambda\|^2 \leq \tau^2 K_{bc}(m_{bc})^{-\frac{\beta-1}{\beta+p}}$ for large enough m_{bc} and a positive constant K_{bc} with probability at least $1 - 4e^{-\tau}$ for $\tau \geq 1$. Hence, we can write down the expectation as an integral and split it at $t^* = K_{bc}(m_{bc})^{-\frac{\beta-1}{\beta+p}}$ corresponding to $\tau = 1$:

$$\begin{aligned} \mathbb{E} \|\delta\hat{\mu}_{B|C}^\lambda\|^2 &= \int_0^\infty \mathbb{P}(\|\delta\hat{\mu}_{B|C}^\lambda\|^2 \geq t) dt \\ &= \int_0^{t^*} \mathbb{P}(\|\delta\hat{\mu}_{B|C}^\lambda\|^2 \geq t) dt + \int_{t^*}^\infty \mathbb{P}(\|\delta\hat{\mu}_{B|C}^\lambda\|^2 \geq t) dt \\ &\leq \int_0^{t^*} 1 dt + \int_{t^*}^\infty 4 \exp\left(-\sqrt{t \frac{1}{K_{bc}} m_{bc}^{\frac{\beta-1}{\beta+p}}}\right) dt = 9 K_{bc} m_{bc}^{-\frac{\beta-1}{\beta+p}}. \end{aligned}$$

By the exact same argument, and using the bias-variance decomposition of the bound (Eq. 12 of Li et al. (2022b) and then the proof in Appendix A.3),

$$\mathbb{E} \|\delta\hat{\mu}_{A|C}^\lambda\|^2 \leq \|\delta\mu_{A|C}^\lambda\|^2 + 9 K_{ac} m_{ac}^{-\frac{\beta-1}{\beta+p}}. \quad (15)$$

Finally, by Lemma 1 of A.1 Li et al. (2022b), we have a (deterministic) bound (note a different HS norm defined by the β interpolation space; the standard norm corresponds to $\beta = 1$; see more details in Li et al. (2022b)):

$$\|\delta\mu_{A|C}^\lambda\|^2 \leq \|\mu_{A|C}\|_\beta^2 \lambda^{\beta-1} = \|\mu_{A|C}\|_\beta^2 m_{ac}^{-\frac{\beta-1}{\beta+p}}$$

where we used the optimal learning rate $\lambda = m_{ac}^{-\frac{1}{\beta+p}}$.

It remains to compare the bias in KCI for the full train set and SplitKCI for halved sets. The constant K_{ac} in Eq. (15) is a sum of positive terms, with one of them being $576 A^2 \|\mu_{A|C}\|_\beta^2$, where for the well-specified case of $\alpha = 1$ and A^2 can be defined as the supremum norm of k_y (see Fischer and Steinwart (2020), Theorem 9). Since we assumed that k_y is bounded by one, the KCI bound (Eq. (15)) becomes

$$\begin{aligned} \mathbb{E} \|\delta\hat{\mu}_{A|C}^\lambda\|^2 &\leq \|\mu_{A|C}\|_\beta^2 m_{ac}^{-\frac{\beta-1}{\beta+p}} + 9 \cdot 576 \|\mu_{A|C}\|_\beta^2 m_{ac}^{-\frac{\beta-1}{\beta+p}} + K_1 m_{ac}^{-\frac{\beta-1}{\beta+p}} \\ &= (1 + K_1) \|\mu_{A|C}\|_\beta^2 m_{ac}^{-\frac{\beta-1}{\beta+p}} + K_2 m_{ac}^{-\frac{\beta-1}{\beta+p}}, \end{aligned}$$

for $K_1 = 5184$ and $K_2 > 0$.

For SplitKCI with half the data, we get

$$\begin{aligned} \|\delta\mu_{A|C}^\lambda\|^2 &\leq \|\mu_{A|C}\|_\beta^2 \left(\frac{m_{ac}}{2}\right)^{-\frac{\beta-1}{\beta+p}} \leq 2 \|\mu_{A|C}\|_\beta^2 m_{ac}^{-\frac{\beta-1}{\beta+p}}, \\ \|\delta\mu_{B|C}^\lambda\|^2 &\leq \|\mu_{B|C}\|_\beta^2 \left(\frac{m_{bc}}{2}\right)^{-\frac{\beta-1}{\beta+p}} \leq 2 \|\mu_{B|C}\|_\beta^2 m_{bc}^{-\frac{\beta-1}{\beta+p}}. \end{aligned}$$

Combining the bounds and denoting $K_3 = K_{bc}$ for simplicity finishes the proof. \blacksquare

A.3 Wild bootstrap

Theorem 7 (Wild bootstrap) *Assume that m_{ac} and m_{bc} dominate $n^{\frac{\beta+p}{\beta-1}}$ asymptotically for β and p as in Assumption 1, and that k_a , k_b and k_c are bounded by 1. (i) Under the null, $n\hat{V}^*$ and $n\hat{V}$ converge weakly to the same distribution. (ii) Under the alternative, \hat{V}^* converges to zero in probability, and \hat{V} converges to a positive constant.*

Before beginning the proof, we note that in practice we use the unbiased estimator in Eq. (21), which corresponds to a U-statistic. The only difference between the U- and V-statistics of Equations 11 and 21 is essentially removal of the terms $i = j$ in the sum (the scaling is also adapted accordingly). See Kim and Schrab (2023, Lemma 22) for an expression of the difference between U- and V-statistics for the closely-related HSIC case.

Proof We start by setting up the notations. Let

$$\begin{aligned} (K_A^c)_{ij} &= \langle \phi_a(A_i) - \mu_{A|C}(C_i), \phi_a(A_j) - \mu_{A|C}(C_j) \rangle, \\ (\hat{K}_A^c)_{ij} &= \langle \phi_a(A_i) - \hat{\mu}_{A|C}(C_i), \phi_a(A_j) - \hat{\mu}_{A|C}(C_j) \rangle, \end{aligned}$$

and similarly for B instead of A . The V -statistics and wild bootstrap KCI estimates using the true and estimated conditional mean embeddings are given as

$$V = \frac{1}{n^2} \sum_{1 \leq i, j \leq n} (K_A^c)_{ij} (K_C)_{ij} (K_B^c)_{ij}, \quad V^* = \frac{1}{n^2} \sum_{1 \leq i, j \leq n} q_i q_j (K_A^c)_{ij} (K_C)_{ij} (K_B^c)_{ij},$$

$$\hat{V} = \frac{1}{n^2} \sum_{1 \leq i, j \leq n} (\hat{K}_A^c)_{ij} (K_C)_{ij} (\hat{K}_B^c)_{ij}, \quad \hat{V}^* = \frac{1}{n^2} \sum_{1 \leq i, j \leq n} q_i q_j (\hat{K}_A^c)_{ij} (K_C)_{ij} (\hat{K}_B^c)_{ij}.$$

We focus on the KCI case, as the proof for CIRCE follows very similarly (the only difference is that the centered kernel matrix K_A^c is replaced with its non-centered version K_A). The reasoning also applies to SplitKCI. We emphasize that the conditional mean embeddings $\hat{\mu}_{A|C}$, $\hat{\mu}_{B|C}$ do not admit close forms and have to be estimated using the CME estimator (see Equation 8) on *held-out* data.

We prove below that

- (i) under the null $n(\hat{V} - V) \rightarrow 0$ and $n(\hat{V}^* - V^*) \rightarrow 0$ in probability,
- (ii) under the alternative $(\hat{V} - V) \rightarrow 0$ and $(\hat{V}^* - V^*) \rightarrow 0$ in probability.

Before proving (i) and (ii), we first show that they imply the desired results. Chwialkowski et al. (2014) study the wild bootstrap generally and handle the MMD and HSIC as special cases. Similarly to their HSIC setting, a symmetrisation trick can be performed for KCI and CIRCE. We rely on their general results which assume a weaker τ -mixing assumption which is trivially satisfied the i.i.d. setting we consider, we point that similar results can be found in Wu (1986); Shao (2010); Leucht and Neumann (2013).

Under the null, we have

$$n(\hat{V} - \hat{V}^*) = n(\hat{V} - V) + n(V - V^*) + n(V^* - \hat{V}^*)$$

where by (i) $n(\hat{V} - V) \rightarrow 0$ and $n(V^* - \hat{V}^*) \rightarrow 0$ in probability. Chwialkowski et al. (2014, Theorem 1) also guarantees that $n(V - V^*) \rightarrow 0$ weakly. We conclude that $n(\hat{V} - \hat{V}^*) \rightarrow 0$ weakly, that is, $n\hat{V}^*$ and $n\hat{V}$ converge weakly to the same distribution under the null.

Under the alternative, by (ii) we have $(\hat{V} - V) \rightarrow 0$ and $(V^* - \hat{V}^*) \rightarrow 0$ in probability. Moreover, Chwialkowski et al. (2014, Theorems 3 and 2) guarantees that $V^* \rightarrow 0$ in mean squared and that $V \rightarrow c$ in mean squared for some $c > 0$, respectively. We conclude that

$$\hat{V}^* = (\hat{V}^* - V^*) + V^* \rightarrow 0 \quad \text{and} \quad \hat{V} = (\hat{V} - V) + V \rightarrow c$$

in probability. ■

Proof [Proof of (i) and (ii)] This proof adapts the reasoning of Chwialkowski et al. (2014, Lemma 3) for HSIC to hold for KCI. This is particularly challenging because while the mean embedding admits a closed form, the conditional mean embedding does not and has weaker convergence properties (Li et al., 2022b, 2023). We provide results in probability rather than in expectation (one can use Markov's inequality to turn an expected bound into

one holding with high probability). Let us define⁶

$$T_n = \frac{1}{n} \sum_{i=1}^n Q_i (\phi_a(A_i) - \mu_{A|C}(C_i)) \otimes \phi_c(C_i) \otimes (\phi_b(B_i) - \mu_{B|C}(C_i)),$$

$$\widehat{T}_n = \frac{1}{n} \sum_{i=1}^n Q_i (\phi_a(A_i) - \widehat{\mu}_{A|C}(C_i)) \otimes \phi_c(C_i) \otimes (\phi_b(B_i) - \widehat{\mu}_{B|C}(C_i)),$$

where, either $Q_i = q_i$, $i = 1, \dots, n$ Rademacher variable in which case

$$\|T_n\|^2 = \frac{1}{n^2} \sum_{1 \leq i, j \leq n} q_i q_j (K_A^c)_{ij} (K_C)_{ij} (K_B^c)_{ij} = V^* \quad \text{and} \quad \|\widehat{T}_n\|^2 = \widehat{V}^*,$$

or $Q_i = 1$, $i = 1, \dots, n$ in which case $\|T_n\|^2 = V$ and $\|\widehat{T}_n\|^2 = \widehat{V}$. So it suffices to prove

- (i) under the null $n(\|\widehat{T}_n\|^2 - \|T_n\|^2) \rightarrow 0$ in probability,
- (ii) under the alternative $(\|\widehat{T}_n\|^2 - \|T_n\|^2) \rightarrow 0$ in probability.

We can obtain these results provided that

- (iii) $\|\sqrt{n}(\widehat{T}_n - T_n)\| \rightarrow 0$ in probability,

which we prove below. For now, assume (iii) holds.

Under the null, we then have

$$\begin{aligned} n \left| \|\widehat{T}_n\|^2 - \|T_n\|^2 \right| &\leq n \left| \|\widehat{T}_n\| - \|T_n\| \right| \left| \|\widehat{T}_n\| + \|T_n\| \right| \\ &\leq \sqrt{n} \|(\widehat{T}_n - T_n)\| \left(\sqrt{n} \|\widehat{T}_n\| + \sqrt{n} \|T_n\| \right) \\ &\rightarrow 0 \end{aligned}$$

in probability, provided that $\sqrt{n} \|T_n\| < \infty$, which is guaranteed by Chwialkowski et al. (2014, Lemma 4) under the null ($\Delta = 0$ in Lemma 4 notation since we're working with the i.i.d. case), and that $\sqrt{n} \|\widehat{T}_n\| < \infty$, both with arbitrarily high probability. The latter holds since

$$\sqrt{n} \|\widehat{T}_n\| \leq \sqrt{n} \|\widehat{T}_n - T_n\| + \sqrt{n} \|T_n\|$$

where the first term tends to zero due to the assumed m_{ac}, m_{bc} scaling and the second is bounded, with arbitrarily high probability. This proves (i).

Under the alternative, we obtain

$$\begin{aligned} \left| \|\widehat{T}_n\|^2 - \|T_n\|^2 \right| &\leq \left| \|\widehat{T}_n\| - \|T_n\| \right| \left| \|\widehat{T}_n\| + \|T_n\| \right| \\ &\leq \|(\widehat{T}_n - T_n)\| \left(\|\widehat{T}_n\| + \|T_n\| \right) \\ &\rightarrow 0 \end{aligned}$$

6. Note that the scaling is different from Chwialkowski et al. (2014, Equation 7).

in probability, as $\|T_n\| < \infty$ by bounding the kernels and the Q_i 's by 1, and

$$\|\widehat{T}_n\| \leq \sqrt{n} \|\widehat{T}_n - T_n\| + \|T_n\|$$

with again the first term tending to zero and the second one being bounded, with arbitrarily high probability. This proves (ii). \blacksquare

Proof [Proof of (iii)] Li et al. (2023, Theorem 2.2.a), with $\gamma = 1$, $\beta \in (1, 2]$, $\alpha = 1$ (see Assumption 1), provides a rate of convergence in RKHS norm for the CME estimator when the true conditional mean embedding lies within a β -smooth subset of the RKHS ($\beta = 1$ would correspond to the full RKHS). There exists a constant $C > 0$ independent of m_{ac} and τ such that

$$\|\widehat{\mu}_{A|C} - \mu_{A|C}\| \leq C\tau m_{ac}^{-\frac{\beta-1}{2(\beta+p)}} \quad \text{with probability at least } 1 - 5e^{-\tau}$$

for m_{ac} sufficiently large and for all $\tau > \ln(5)$, where $p \in (0, 1]$ induces a smoothness condition on the kernel used (its eigenvalues μ_i must decay as $i^{-1/p}$). As justified below, we will be interested in the scaled rate

$$\|\sqrt{n}(\widehat{\mu}_{A|C} - \mu_{A|C})\| \leq C\tau n^{\frac{1}{2}} m_{ac}^{-\frac{\beta-1}{2(\beta+p)}}.$$

Now, assuming that $m_{ac} = \omega(n^{\frac{\beta+p}{\beta-1}})$ (i.e. m_{ac} dominates $n^{\frac{\beta+p}{\beta-1}}$ asymptotically), then we obtain

$$\|\sqrt{n}(\widehat{\mu}_{A|C} - \mu_{A|C})\| \rightarrow 0 \tag{16}$$

in probability as n tends to infinity. Note that this trivially implies that

$$\|\widehat{\mu}_{A|C}\| \leq \|\sqrt{n}(\widehat{\mu}_{A|C} - \mu_{A|C})\| + \|\mu_{A|C}\| < \infty \tag{17}$$

for all $n \in \mathbb{N}$. The results in Equations (16 and 17) also hold using B instead of A .

We are now ready to show that $\|\sqrt{n}(\widehat{T}_n - T_n)\| \rightarrow 0$ in probability. Note that

$$\begin{aligned} \sqrt{n}(\widehat{T}_n - T_n) &= \frac{1}{\sqrt{n}} \sum_{i=1}^n Q_i \left((\phi_a(A_i) - \widehat{\mu}_{A|C}(C_i)) \otimes \phi_c(C_i) \otimes (\phi_b(B_i) - \widehat{\mu}_{B|C}(C_i)) \right. \\ &\quad \left. - (\phi_a(A_i) - \mu_{A|C}(C_i)) \otimes \phi_c(C_i) \otimes (\phi_b(B_i) - \mu_{B|C}(C_i)) \right) \end{aligned} \tag{18}$$

$$= \frac{1}{\sqrt{n}} \sum_{i=1}^n Q_i \phi_a(A_i) \otimes \phi_c(C_i) \otimes \left(\mu_{B|C}(C_i) - \widehat{\mu}_{B|C}(C_i) \right) \tag{19}$$

$$\begin{aligned} &+ \frac{1}{\sqrt{n}} \sum_{i=1}^n Q_i \left(\mu_{A|C}(C_i) - \widehat{\mu}_{A|C}(C_i) \right) \otimes \phi_c(C_i) \otimes \phi_b(B_i) \\ &+ \frac{1}{\sqrt{n}} \sum_{i=1}^n Q_i \left(\widehat{\mu}_{A|C}(C_i) \otimes \phi_c(C_i) \otimes \widehat{\mu}_{B|C}(C_i) - \mu_{A|C}(C_i) \otimes \phi_c(C_i) \otimes \mu_{B|C}(C_i) \right). \end{aligned} \tag{20}$$

The terms (18) and (19) can be handled in a similar fashion, the term (20) needs to be tackle separately. Note that in the CIRCE case we would have only the first term (18).

The term (18) is

$$\begin{aligned}
& \left\| \frac{1}{\sqrt{n}} \sum_{i=1}^n Q_i \phi_a(A_i) \otimes \phi_c(C_i) \otimes \left(\mu_{B|C}(C_i) - \hat{\mu}_{B|C}(C_i) \right) \right\| \\
& \leq \frac{1}{n} \sum_{i=1}^n |Q_i| \left\| \phi_a(A_i) \otimes \phi_c(C_i) \otimes \sqrt{n} \left(\mu_{B|C}(C_i) - \hat{\mu}_{B|C}(C_i) \right) \right\| \\
& = \frac{1}{n} \sum_{i=1}^n (k_a(A_i, A_i) k_c(C_i, C_i))^{1/2} \left\| \sqrt{n} \left(\mu_{B|C}(C_i) - \hat{\mu}_{B|C}(C_i) \right) \right\| \\
& \leq \frac{1}{n} \sum_{i=1}^n k_a(A_i, A_i)^{1/2} k_c(C_i, C_i) \left\| \sqrt{n} \left(\mu_{B|C} - \hat{\mu}_{B|C} \right) \right\|_{\text{HS}} \\
& \leq \left\| \sqrt{n} \left(\mu_{B|C} - \hat{\mu}_{B|C} \right) \right\| \\
& \rightarrow 0
\end{aligned}$$

in probability by Equation (16), where we the triangle inequality (2nd line), product space definition (3rd line), $\|\mu_{A|C}(c)\| \leq \|\mu_{A|C}\| k_c(c, c)^{1/2}$ (4th line) and the facts that k_a , k_c and Q_i are all bounded by 1.

Similarly, the second term (19) converges to 0 in probability.

For the third term (20), we have

$$\begin{aligned}
& \left\| \frac{1}{\sqrt{n}} \sum_{i=1}^n Q_i \left(\hat{\mu}_{A|C}(C_i) \otimes \phi_c(C_i) \otimes \hat{\mu}_{B|C}(C_i) - \mu_{A|C}(C_i) \otimes \phi_c(C_i) \otimes \mu_{B|C}(C_i) \right) \right\| \\
& \leq \frac{1}{n} \sum_{i=1}^n |Q_i| \left\| \sqrt{n} \left(\hat{\mu}_{A|C}(C_i) \otimes \phi_c(C_i) \otimes \hat{\mu}_{B|C}(C_i) - \mu_{A|C}(C_i) \otimes \phi_c(C_i) \otimes \mu_{B|C}(C_i) \right) \right\| \\
& = \frac{1}{n} \sum_{i=1}^n \sqrt{k_c(C_i, C_i)} \left\| \sqrt{n} \left(\hat{\mu}_{A|C}(C_i) \otimes (\hat{\mu}_{B|C}(C_i) \pm \mu_{B|C}(C_i)) - \mu_{A|C}(C_i) \otimes \mu_{B|C}(C_i) \right) \right\| \\
& \leq \frac{1}{n} \sum_{i=1}^n \sqrt{k_c(C_i, C_i)} \left(\left\| \sqrt{n} \hat{\mu}_{A|C}(C_i) \otimes (\hat{\mu}_{B|C}(C_i) - \mu_{B|C}(C_i)) \right\| + \right. \\
& \quad \left. \left\| \sqrt{n} (\hat{\mu}_{A|C}(C_i) - \mu_{A|C}(C_i)) \otimes \mu_{B|C}(C_i) \right\| \right) \\
& = \frac{1}{n} \sum_{i=1}^n \sqrt{k_c(C_i, C_i)} \left(\left\| \hat{\mu}_{A|C}(C_i) \right\| \left\| \sqrt{n} (\hat{\mu}_{B|C}(C_i) - \mu_{B|C}(C_i)) \right\| + \right. \\
& \quad \left. \left\| \mu_{B|C}(C_i) \right\| \left\| \sqrt{n} (\hat{\mu}_{A|C}(C_i) - \mu_{A|C}(C_i)) \right\| \right) \\
& \leq \frac{1}{n} \sum_{i=1}^n (k_c(C_i, C_i))^{3/2} \left(\left\| \hat{\mu}_{A|C} \right\| \left\| \sqrt{n} (\hat{\mu}_{B|C} - \mu_{B|C}) \right\| + \left\| \mu_{B|C} \right\| \left\| \sqrt{n} (\hat{\mu}_{A|C} - \mu_{A|C}) \right\| \right) \\
& \leq \left\| \hat{\mu}_{A|C} \right\| \left\| \sqrt{n} (\hat{\mu}_{B|C} - \mu_{B|C}) \right\| + \left\| \mu_{B|C} \right\| \left\| \sqrt{n} (\hat{\mu}_{A|C} - \mu_{A|C}) \right\| \\
& \rightarrow 0
\end{aligned}$$

in probability by Equation (16), using the triangle inequality (second line), product spaces definition (third line), again triangle inequality (4th) and product spaces definition (5th) and then $\|\mu_{A|C}(c)\| \leq \|\mu_{A|C}\| k_c(c, c)^{1/2}$ and the fact that $k_c(c, c)$ and Q_i are bounded by 1, with the final result holding since $\|\widehat{\mu}_{A|C}\| < \infty$ by Equation (17).

We deduct that $\|\sqrt{n}(\widehat{T}_n - T_n)\| \rightarrow 0$ in probability, which shows (iii).

This concludes the proof of Theorem 7. \blacksquare

Appendix B. Measures of conditional independence

B.1 Kernel ridge regression

For completeness, we include the kernel ridge regression algorithm with leave-one-out error (for RKHS-valued outputs, see Pogodin et al., 2022) in Algorithm 2. While it is possible to optimize the LOO errors via gradient descent over λ and kernel parameters, in practice this can be computationally demanding. In our experiments, we choose the parameters over a pre-defined grid.

Data: $\{(x_i, y_i)\}_{i=1}^m$

Parameter selection:

Fixed \mathcal{H}_y

Optimised $\lambda > 0$ and \mathcal{H}_x^* over a set of $\{\mathcal{H}_x\}$ with leave-one-out:

$$\mathcal{H}_x^*, \lambda^* = \arg \min_{\mathcal{H}_x, \lambda} \text{LOO}(\mathcal{H}_x, \lambda)$$

$$\text{LOO}(\mathcal{H}_x, \lambda) = \sum_{i=1}^m \frac{\|\phi_y(y_i) - K_{x_i X} (K_X + \lambda m I)^{-1} \Phi_Y\|_{\mathcal{H}_y}^2}{(1 - (K_X (K_X + \lambda m I))_{ii})^2}$$

Result: $\widehat{\mu}_{Y|X}(x) = K_{x X} (K_X + \lambda m I_m)^{-1} \Phi_Y$ # Eq. (8)

Algorithm 2: Kernel ridge regression with leave-one-out (LOO) hyperparameter search.

Here K_X and $K_{x X}$ are computed for each \mathcal{H}_x during LOO and then re-computed for \mathcal{H}_x^* .

B.2 KCI

Notes on the original implementation First, we note that the set $E'_1 = \{g \in L_A^2 : \mathbb{E}[g(A) | C] = 0\}$ used in the original KCI formulation (Zhang et al., 2011) is not present in Theorem 1 of Daudin (1980). The theorem is proven for $E_1 = \{g \in L_{AC}^2 : \mathbb{E}[g(A, C) | C] = 0\}$, and stated for $g \in L_{AC}^2$ and $g \in L_A^2$. However, we note that E'_1 functions can be constructed as $g = g' - \mathbb{E}[g' | C]$ for $g' \in L_A^2$. Therefore, given $h \in \{h \in L_{BC}^2 : \mathbb{E}[h(B, C) | C] = 0\}$, we have $\mathbb{E}[gh] = 0$ iff $\mathbb{E}[g'h] = 0$ since $\mathbb{E}[\mathbb{E}[g' | C]h(B, C)] = \mathbb{E}[\mathbb{E}[g' | C]\mathbb{E}[h(B, C) | C]] = 0$. Therefore, the proof for this case follows the $g \in L_A^2$ case of Daudin (1980) (see Corollary A.3 of Pogodin et al. 2022 for the required proof).

Second, the original KCI definition estimated the $\phi_{bc}(B, C) - \mu_{BC|C}(C)$ residual. For radial basis kernels, this can be decomposed into $\phi_c(C) \otimes (\phi_b - \mu_{B|C})$, avoiding estimation of $\mu_{C|C} = \phi_c(C)$ (see Pogodin et al., 2022). This is crucial to ensure consistency of the regression, because estimating $\mu_{C|C}$ is equivalent to estimating the identity operator — for a characteristic RKHS \mathcal{H}_c , this operator is not Hilbert-Schmidt and thus the regression problem is not well-specified. This is described in Appendix B.9 of Mastouri et al. (2021) (also see Appendix D, $Y = X$ case, of Li et al. 2022b). In practice, computing the $C \rightarrow C$

regression can lead to significant problems, as described by Mastouri et al. (2021, Appendix B.9 and Figure 4). For 1d Gaussian C , the CME estimator correctly estimates the identity on the high density regions of the training data; in the tail of the distribution, however, the estimate becomes heavily biased since those points are rarely present in the training data.

Gamma approximation for KCI The Gamma approximation of p -values was used by Zhang et al. (2011) (and previously suggested for independence testing with HSIC by Gretton et al. 2007). This approximation uses the fact that under the null, the kernel-based statistics are distributed as a weighted (infinite) sum of χ^2 variables $\sum \lambda_i \xi_i^2$ for $\xi_i \sim \mathcal{N}(0, 1)$. While this sum is intractable, it can be approximated as a Gamma distribution $p(t) = t^{k-1} \frac{e^{-t/\theta}}{\theta^k \gamma(k)}$ with parameters (for the KCI estimator $\frac{1}{n^2} \text{Tr}(KL)$ with centered matrices K and L) estimated as

$$\mu = \frac{1}{n} \sum_{i=1}^n K_{ii} L_{ii}, \quad \sigma^2 = 2 \frac{1}{n^2} \sum_{i,j} K_{ij}^2 L_{ij}^2, \quad k = \frac{\mu}{\sigma^2}, \quad \theta = \frac{\sigma^2}{n \mu}.$$

The Gamma approximation is not exact, and higher-order moment matching methods can improve approximation quality (Bodenham and Adams, 2016). In our tests with KCI and its variants, the Gamma approximation produced p -values that are consistently lower than the required level under H_0 (Fig. 10, left for wild bootstrap vs. right for Gamma approximation). This might be attributed not to the approximation itself (e.g. it performed well in (Gretton et al., 2007; Zhang et al., 2011)) but rather to large CME estimation errors in our tasks that introduce bias in mean/variance estimation for the method. For CIRCE, the situation was reversed, which could also be potentially explained by (the lack of) CME estimation bias in one of its terms.

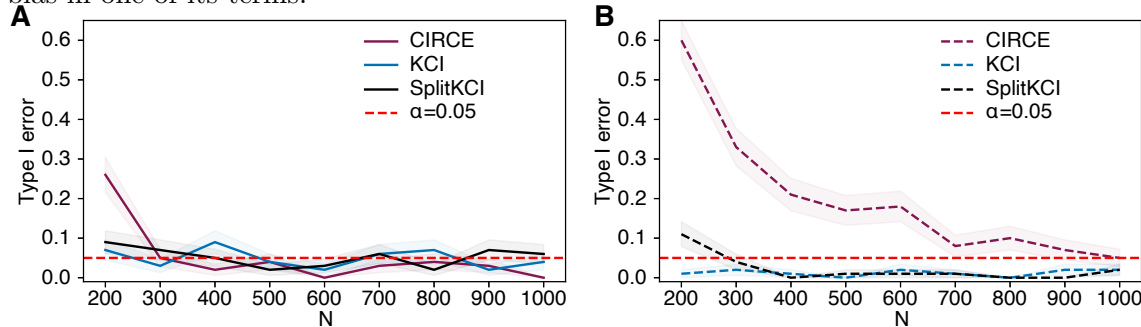


Figure 10: Type I error comparison between **A.** wild bootstrap and **B.** the Gamma approximation methods of p -value estimation for Gaussian data (see Section C.1). Lines/shaded area: mean/±SE over 100 trials, $\alpha = 0.05$.

For SplitKCI, we use the train/test splitting procedure outlined in Section 5.2. See Algorithm 3 for a more detailed description. Note that this can be viewed as testing with the CIRCE operator (6), in which we test $C \perp\!\!\!\perp A | C$, where the kernel over the conditioning variable is just $k_c(c, c') = 1$.

Data: $\mathcal{D} = \{(a_i, b_i, c_i)\}_{i=1}^N$, test size ratio grid $[\beta_1, \dots, \beta_k]$, target rejection rate α , number of test resamples r

```

reject_rate = 1
for β in [β_k, ..., β_1] (decreasing):
    if reject_rate ≤ α:
        return β
    reject_rate = 0
    for i in [1, ..., r]:
        Random  $\mathcal{D}_{\text{train}}^m, \mathcal{D}_{\text{test}}^n$  with  $n = \beta N, m = (1 - \beta)N$ 
         $p_A$  obtained from Algorithm 1 with  $\mathcal{D}_{\text{train}}^m, \mathcal{D}_{\text{test}}^n$  and  $K_B^c = I$ 
         $p_B$  obtained from Algorithm 1 with  $\mathcal{D}_{\text{train}}^m, \mathcal{D}_{\text{test}}^n$  and  $K_A^c = I$ 
        reject_rate = reject_rate +  $\frac{1}{r} ((p_A \leq \alpha) \& (p_B \leq \alpha))$ 

```

Algorithm 3: Train/test split selection algorithm.

B.3 GCM

The Generalised Covariance Measure (GCM, Shah and Peters, 2020) relies on estimates of the conditional mean

$$\hat{f}(C) \approx \mathbb{E}[A | C], \quad \hat{g}(C) \approx \mathbb{E}[B | C].$$

For n samples $a_i \in \mathbb{R}^{d_a}$ and $b_i \in \mathbb{R}^{d_b}$, define

$$R_{ikl} = (a_i - \hat{f}(c_i))_k (b_i - \hat{g}(c_i))_l, \quad \bar{R}_{kl} = \frac{1}{n} \sum_{i=1}^n R_{ikl}, \quad T_{kl} = \frac{\sqrt{n} \bar{R}_{kl}}{\sqrt{\frac{1}{n} \sum_{j=1}^n (R_{jl})^2 - (\bar{R}_{kl})^2}}.$$

For 1-dimensional A and B (and arbitrary C), the p -value is computed as $p = 2(1 - \Phi(|T_{11}|))$ for the standard normal CDF Φ .

For higher-dimensional A and B (with $d_a d_b \geq 3$), the statistic becomes $S = \max_{k,l} |T_{kl}|$, and the p -value is computed by approximating the null distribution of T_{kl} as a zero-mean Gaussian with the covariance matrix (for a n -dimensional vector R^{kl} corresponding to all data points and dimensions k, l)

$$\Sigma_{kl,pd} = \frac{\frac{1}{n} \sum_{i=1}^n R_{ikl} R_{ipd} - \bar{R}_{kl} \bar{R}_{pd}}{\sqrt{\frac{1}{n} \sum_{i=1}^n R_{ikl}^2 - \bar{R}_{kl}^2} \sqrt{\frac{1}{n} \sum_{i=1}^n R_{ipd}^2 - \bar{R}_{pd}^2}}.$$

B.4 RBPT2

The Rao-Blackwellized Predictor Test (Polo et al., 2023; “2” stands for the test variant that doesn’t require approximation of $P(B | C)$) first trains a predictor $g(B, C)$ of A , e.g. by computing $g(B, C) \approx \mathbb{E}[A | B, C]$. (The original paper used a linear regression; we test this setup and also a CME with a Gaussian kernel.) Then, it builds a second predictor through CME as $h(C) = \mathbb{E}[g(B, C) | C]$ (the original paper used a polynomial kernel of degree two; we obtain similar results for a Gaussian kernel for linear g and a set of Gaussian/polynomial kernels for a Gaussian g). Then, for a convex loss l , the test statistic S is computed as

$$T_i = l(h(c_i), a_i) - l(g(b_i, c_i), a_i), \quad S = \frac{\sqrt{n} \sum_{i=1}^n T_i}{\sqrt{\sum_{i=1}^n T_i^2 - (\sum_{i=1}^n T_i)^2}}.$$

The p -value is then computed as $p = 1 - \Phi(S)$ (one-sided test); the basic intuition is that if B has no extra information about A apart from the joint C -dependence, the second predictor h will perform as well as the first one g .

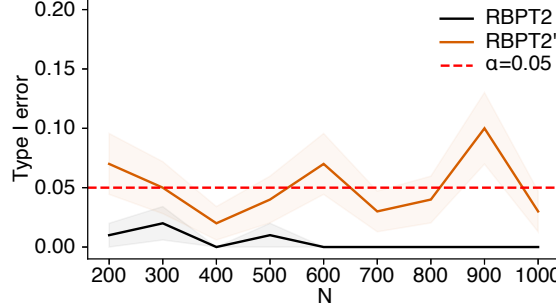


Figure 11: Type I error comparison between RBPT2 (black) vs its unbiased version RBPT2' (orange) for Gaussian data (see Section C.1). Lines/shaded area: mean/ \pm SE over 100 trials, $\alpha = 0.05$.

For Polo et al. (2023), the loss (for one-dimensional A, B) was the mean squared error loss $l(g, a) = (g - a)^2$. For d_a -dimensional a , we also used the MSE loss $l(g, a) = \|g - a\|_2^2$ and found the test to consistently produce much lower Type I error than the nominal level α . We show an example of this behaviour for Gaussian data in Fig. 11 (black line); for the RatInABox task in the same setup as in Fig. 6, the test would always reject regardless of the ground truth (not shown). This indicates that the statistic S doesn't follow a standard normal distribution. We argue that this happens due to the CME estimation error, and propose a debiased version of RBPT2 (which computes correct p -values; Fig. 11, orange line):

Theorem 8 Denote the approximation error of $\mathbb{E}[A | B, C]$ via $g(B, C)$ as δg :

$$g(B, C) = \mathbb{E}[A | B, C] + \delta g(B, C).$$

Assume that the second regression h uses much more data (i.e. the unbalanced data regime in the main text) and so correctly estimates $h = \mathbb{E}[g(B, C) | C]$, and that RBPT2 uses the MSE loss l .

Then, under H_0 , the unnormalized test statistic $T(A, B, C) = \|h(C) - A\|_2^2 - \|g(B, C) - A\|_2^2$ has a negative bias:

$$\mathbb{E}[T(A, B, C)] =_{H_0} -\mathbb{E}[\|g(B, C) - h(C)\|_2^2].$$

Proof Under H_0 , we have that

$$\begin{aligned} g(B, C) &= \mu_{A|BC}(B, C) + \delta g(B, C) =_{H_0} \mu_{A|C}(C) + \delta g(B, C), \\ h(C) &= \mu_{A|C}(C) + \mathbb{E}[\delta g(B, C) | C] = \mu_{A|C}(C) + \mu_{\delta g}(C). \end{aligned}$$

We can therefore decompose the loss difference as

$$\begin{aligned} \|h(C) - A\|_2^2 - \|g(B, C) - A\|_2^2 &=_{H_0} \|\mu_{A|C}(C) - A + \mu_{\delta g}(C)\|_2^2 - \|\mu_{A|C}(C) - A + \delta g(B, C)\|_2^2 \\ &= 2(\mu_{A|C}(C) - A)^\top \mu_{\delta g}(C) + \|\mu_{\delta g}(C)\|_2^2 - 2(\mu_{A|C}(C) - A)^\top \delta g(B, C) - \|\delta g(B, C)\|_2^2. \end{aligned}$$

We can take the expectation of this difference under H_0 , zeroing out the cross-product terms since $A \perp\!\!\!\perp B | C$:

$$\begin{aligned}\mathbb{E} [\|h(C) - A\|_2^2 - \|g(B, C) - A\|_2^2] &=_{H_0} -\mathbb{E} [\|\delta g(B, C)\|_2^2 - \|\mu_{\delta g}(C)\|_2^2] \\ &= -\mathbb{E} [\|\delta g(B, C) - \mu_{\delta g}(C)\|_2^2] = -\mathbb{E} [\|g(B, C) - h(C)\|_2^2].\end{aligned}$$

■

Conveniently, we can estimate this bias from the g, h estimates, resulting in a bias-corrected RBPT2 (called RBPT2' in the main text) with a test statistic

$$T_i = \|h(c_i) - a_i\|_2^2 - \|g(b_i, c_i) - a_i\|_2^2 + \|g(b_i, c_i) - h(c_i)\|_2^2.$$

While the derivation holds under the null, we note that adding a positive term to T_i should decrease Type II errors since we're testing for large positive deviations in T_i .

Appendix C. Experimental details and additional experiments

In all cases, we ran wild bootstrap 1000 times to estimate p -values. For kernel ridge regression, the λ values were chosen (via leave-one-out) from $[10\delta, \dots, 10^7\delta]$ (log scale) for SVD tolerance $\delta = \|K_C\|_2 \epsilon$ and machine precision ϵ (for `float32` values).

For the experiments with the post-nonlinear model (Section 7.3) and the additional synthetic task (Section C.1) with KCI, SplitKCI, and CIRCE, the kernels over A and B were Gaussian $k(x, x') = \exp(-\|x - x'\|_2^2/\sigma^2)$ (note that σ^2 is not multiplied by two in our implementation) with $\sigma^2 = 1$ as the data was normalized. The kernel over C for $\mu_{B|C}$ was always Gaussian, with σ^2 chosen (via leave-one-out) from $[0.1, 0.2, 0.5, 1.0, 1.5, 2.0]$. For GCM, we use the same setup for $\hat{f}(C) \approx \mathbb{E}[A|C]$, $\hat{g}(C) \approx \mathbb{E}[B|C]$ (see the definitions in Section B.3). For RBPT2, we used the linear kernel for $g(B, C)$ and the Gaussian kernel for $h(C)$ with the same parameter choice as for $\hat{\mu}_{A|C}$ (see the definitions in Section B.4).

For the synthetic rat data experiments and KCI-style methods, the kernels over A and B remained the same. For C , we parametrized the Gaussian kernel as $k(x, x') = \exp(-\sum_{i=1}^d (x_i - x'_i)^2 \gamma_i^2 / d)$. For $\hat{\mu}_{B|C}$, we chose $\gamma_i = \gamma$ (the same for all i) from $[0.1, 0.2, 0.5, 1.0, 1.5, 2.0]$. For $\hat{\mu}_{A|C}$, we additionally chose from $\gamma_1 = \gamma_2 = 0$ and $\gamma_3 = \gamma_4 = 0$ options (no head direction/no position coordinates) with $d = 2$ in those cases. As A only depends on head direction, such features selection improves regression error. The same approach was used for GCM. For RBPT, we used the Gaussian kernel with $\sigma^2 = 1$ for g ; for h , we used the same kernel as for $\hat{\mu}_{A|C}$. This was done to reflect the increased model flexibility in other measures; in the original experiments of Polo et al. (2023), g was found through (non-ridge) regression and h used a polynomial kernel of degree 2. We found this setup to be similar to our first setup in our preliminary experiments (not shown).

For all synthetic data experiments, we used 100 random seeds, plotting plotted mean \pm SE for the error rates. The train/test splitting procedure for SplitKCI (Algorithm 3) used $\alpha = 0.5$ and test ratio β ranging from 0.1 to 0.5, such that $\beta N \geq \max(100, 0.1 N)$ with a step of βN of 50.

For the car insurance data, we followed exactly the same procedure as Polo et al. (2023) for RBPT, RBPT2, RBPT2' and GCM. For kernel-based measures and the simulated H_0 , the kernel over A was Gaussian with σ^2 determined from sample variance over train data;

the kernel over B was a simple $k_b(b, b') = \mathbb{I}[b = b']$ since B is binary; the kernel over C was Gaussian with σ^2 chosen from $[0.5, 1.0, 2.0] \cdot \hat{\sigma}^2$ for train sample variance $\hat{\sigma}^2$. For the actual p -values, we split the train data in two randomly for independent $\mu_{A|C}$ and $\mu_{B|C}$ regression (to avoid the high memory requirements of the full dataset). The rejection indicators p_{ij} for seed i for the simulated H_0 task were computed for each company j individually. As in Polo et al. (2023), we did not make the variance correction through the law of total variance, essentially estimating average rejection rate across companies, since the companies are fixed and not sampled randomly. Therefore, the standard errors are correct (for this quantity).

For KCI, CIRCE and SplitKCI with the Gamma approximation, we used the biased HSIC-like estimator in Eq. (11) (note that the Gamma approximation is derived for the biased one). For wild bootstrap, we used the unbiased HSIC estimator (Song et al., 2007) (the biased one performed marginally worse; not shown) for kernel matrices K, L :

$$\frac{1}{m(m-3)} \left(\text{Tr} (KL) + \frac{1^\top K 1 1^\top L 1}{(m-1)(m-2)} - \frac{2}{m-2} 1^\top K L 1 \right). \quad (21)$$

C.1 Additional toy task

We sample a circular C with A and B being noisy version of C , with conditional dependence along the first coordinate under H_1 . For H_0 ,

$$C = \frac{\xi_1}{\|\xi_1\|_2}, \quad A = C + \gamma \xi_2 + \gamma \xi_a, \quad B = C + \gamma \xi_3 + \gamma \xi_b.$$

For H_1 , part of the noise in A and B is shared through ξ_{ab} ,

$$C = \frac{\xi_1}{\|\xi_1\|_2}, \quad A = C + \gamma \xi_2 + \gamma \begin{bmatrix} \xi_{ab} \\ \xi_{aa} \end{bmatrix}, \quad B = C + \gamma \xi_3 + \gamma \begin{bmatrix} \xi_{ab} \\ \xi_{bb} \end{bmatrix},$$

where $\xi_1, \xi_2, \xi_3, \xi_a, \xi_b \sim \mathcal{N}(0, I_2)$, $\xi_{ab}, \xi_{aa}, \xi_{bb} \sim \mathcal{N}(0, 1)$ and for $\gamma = 0.05$.

For both Figs. 10 and 11, we varied the total budget from $N = 200$ to $N = 1000$, always using 100 points for testing and the rest for training.

C.2 Post-nonlinear model

In addition to the main results in Sections 7.2 and 7.3, we evaluated all methods (including CIRCE) without train/test splitting (Fig. 12) and with a fixed split of $n = 100$ test points (Fig. 13). In all cases, CIRCE showed trivial results (almost perfect Type I error but also Type II error close to 1, meaning that it would mostly just reject the alternative). RBPT' suffered from not having a train/test split, while KCI and SplitKCI, in contrast, worked well even without a split on this task.

C.3 Synthetic neural data

To generate the data, we used the RatInABox toolbox (MIT license) George et al. (2024). We used a rectangular box with four walls blocking the central part of the box, so the simulated rat runs in circles around the center. This adds a marginal dependence between head direction and position.

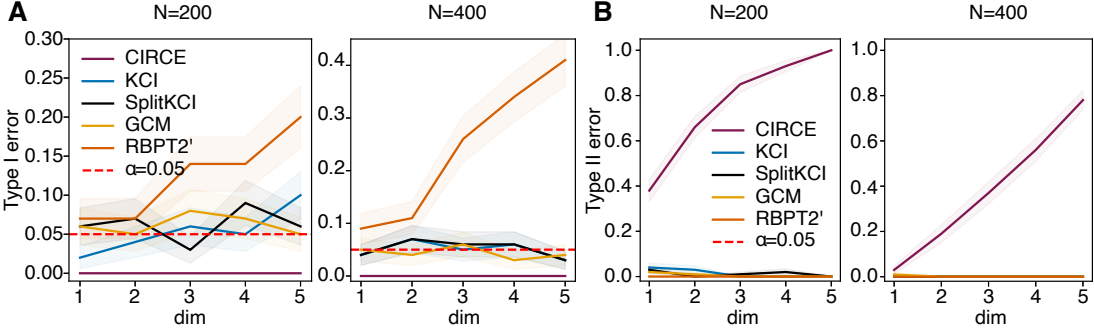


Figure 12: Post-nonlinear model experiments for increasing dimensionality of the task. Unlike in Fig. 3, all methods use all data points for both testing and training. **A.** Type I error for $N = 200$ (left) and $N = 400$ (right) data points. **B.** Type II error for $N = 200$ (left) and $N = 400$ (right) data points. Lines/shaded area: mean/ \pm SE over 100 trials, $\alpha = 0.05$.

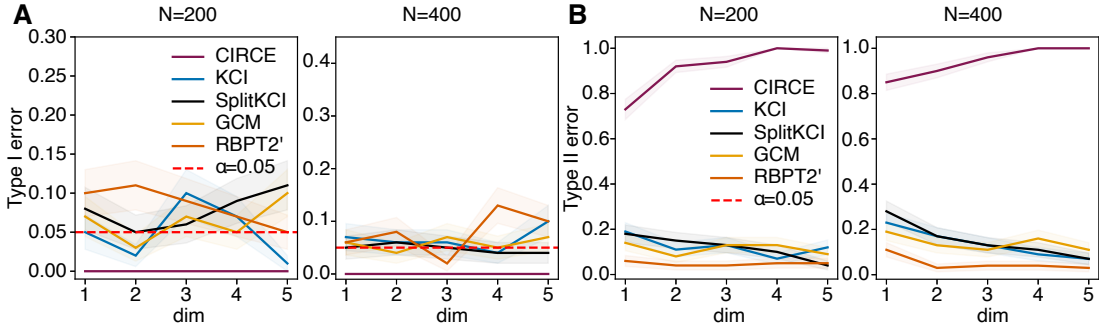


Figure 13: Post-nonlinear model experiments for increasing dimensionality of the task. Unlike in Fig. 3, all methods use 100 data points for testing and the rest for training. **A.** Type I error for $N = 200$ (left) and $N = 400$ (right) data points. **B.** Type II error for $N = 200$ (left) and $N = 400$ (right) data points. Lines/shaded area: mean/ \pm SE over 100 trials, $\alpha = 0.05$.

We then simulated 100 head directional cells A and 100 grid cells B with their underlying firing rate $r_a(t), r_b(t)$ bounded between 0 and 1 Hz, an Ornstein–Uhlenbeck (OU) process $\xi_a(t), \xi_b(t)$ with 0.1 std and a fast time constant. The observed firing rate for head directional cells was $\hat{r}_a(t) = \text{ReLU}(r_a(t) + \xi_a(t))$. Under the null, we constructed conjunctive cells from grid cells B and an independent set of head directional cells A' as $\hat{r}_b(t) = \text{ReLU}(\hat{r}_{a'}(t) + r_b(t) + \xi_b(t))$. Under the alternative, we constructed the conjunctive cells as $\hat{r}_b(t) = \text{ReLU}(\hat{r}_{a'}(t) + r_b(t) + \xi_b(t) - 1)$ (-1 makes sure the cells are active only when both the head direction and position are correct). We simulated the rat for several minutes for each random seed, subsampling the points so the autocorrelation of the OU process is negligible to get approximately i.i.d. data. The exact data generation process is provided in the code.

In the main text, Figs. 6 and 7 show the best performing settings w.r.t. data splits for each presented algorithm, with SplitKCI using the Algorithm 3 to determine the split ratio

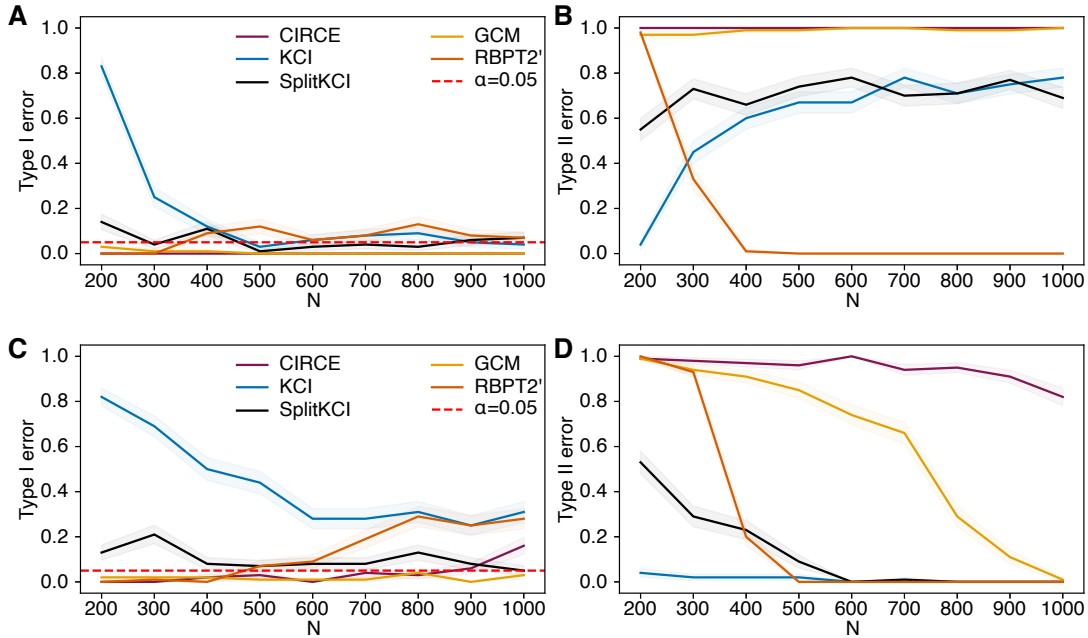


Figure 14: Synthetic neural data experiments for increasing (A, B, C) dataset size. **A.** Type I error for using 100 points (out of N) as test data. **B.** Type II error. **C-D.** Same as **A-B** but for $N/2$ points as test data. Lines/shaded area: mean/ \pm SE over 100 trials, $\alpha = 0.05$.

in the standard data regime. We also evaluated all methods for fixed data splits (Figs. 14 to 17). Omitted in the main text, CIRCE showed reasonable Type I performance along with very poor Type II performance (purple), and SplitKCI without splitting over $\mu_{B|C}$ (Split KCI(A only), green, in the figures) performed very closely to SplitKCI (however, it was sensitive to train/test split ratio and incompatible with our splitting heuristic).

C.3.1 RESULTS WITHOUT TRAIN/TEST SPLITTING

We also evaluated the methods without the train/test splits, i.e. using all data for both training and testing. The results are shown in Fig. 15A-B. As expected, GCM holds level and quickly gains power as the number of points N increases. CIRCE shows pathological performance as it always accepts the null. The other tests struggle to hold level.

To confirm why this is happening, we repeated the same experiment, but now resampling the test sets; see Fig. 15C-D. That is, the number of train/test points was the same as in panels A-B, but the test set was independent of the training one. KCI did not improve performance, showing that the balance of test and train points is indeed important. Interestingly, SplitKCI could hold level for an independent set of points. This could be explained by additional correlations for in-sample errors: if the CME estimation for a given training point is poor for both regressions (i.e. $C \rightarrow A$ and $C \rightarrow B$), it will add a large error term to the test statistic (which is more likely for SplitKCI as it's using fewer points than KCI). For an independent test set, such errors are more likely to be uncorrelated.

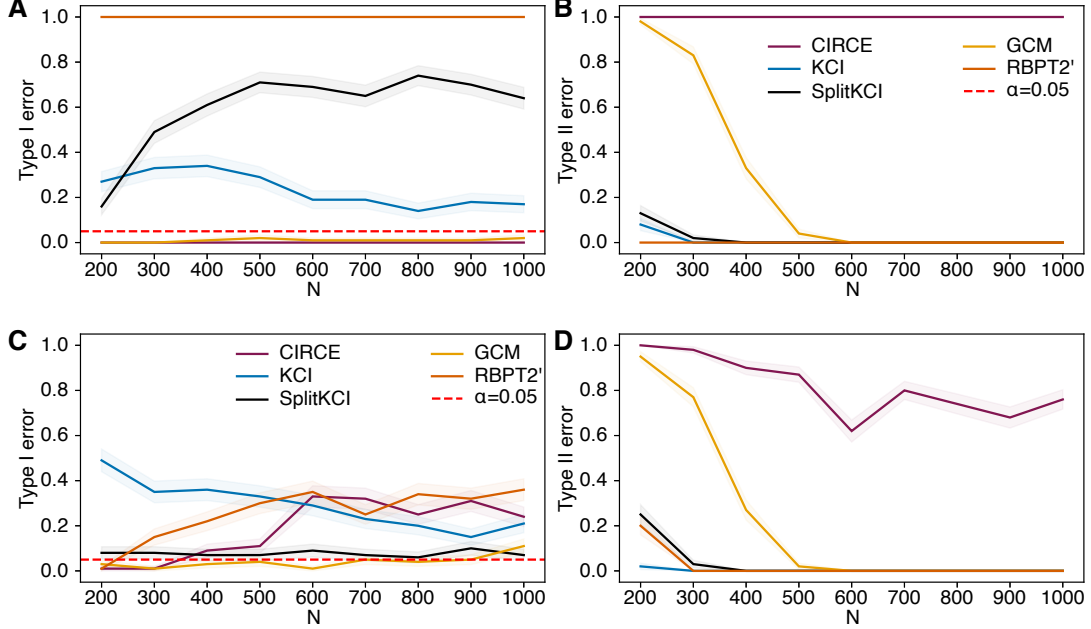


Figure 15: Synthetic neural data experiments for increasing (A, B, C) dataset size. **A.** Type I error without a train/test split (i.e. using the same N points for each part). **B.** Type II error. **C-D.** Same as A-B but for an independent set of N test points (control experiment). Lines/shaded area: mean/ \pm SE over 100 trials, $\alpha = 0.05$.

C.4 Car insurance data

For the car insurance data (full dataset, i.e. merged for all companies), we compute the p -values as in Polo et al. (2023). The train/test split of the dataset is done as 70/30%. For KCI and SplitKCI, we further split the train set in half for each $\mu_{A|C}$ and $\mu_{B|C}$ regression due to increased memory requirements compared to other methods.

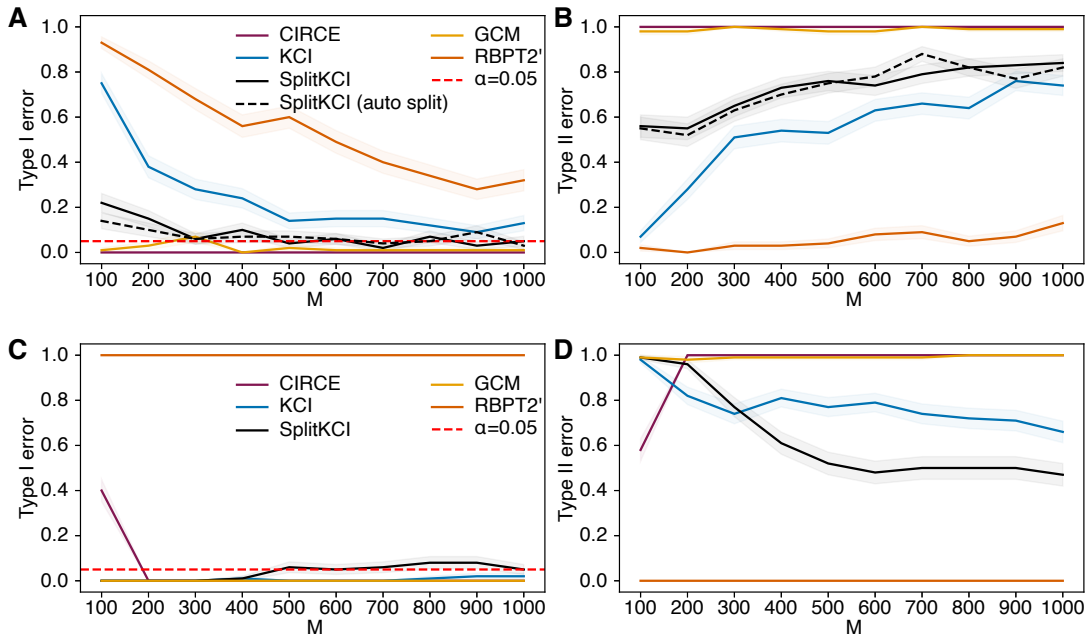


Figure 16: Synthetic neural data experiments for 200 (A, B, C) dataset size, but increasing amount of auxiliary (B, C) data. **A.** Type I error for 100/100 train/test split. **B.** Type II error. **C-D.** Same as A-B, but without a train/test split. Lines/shaded area: mean/ \pm SE over 100 trials, $\alpha = 0.05$.

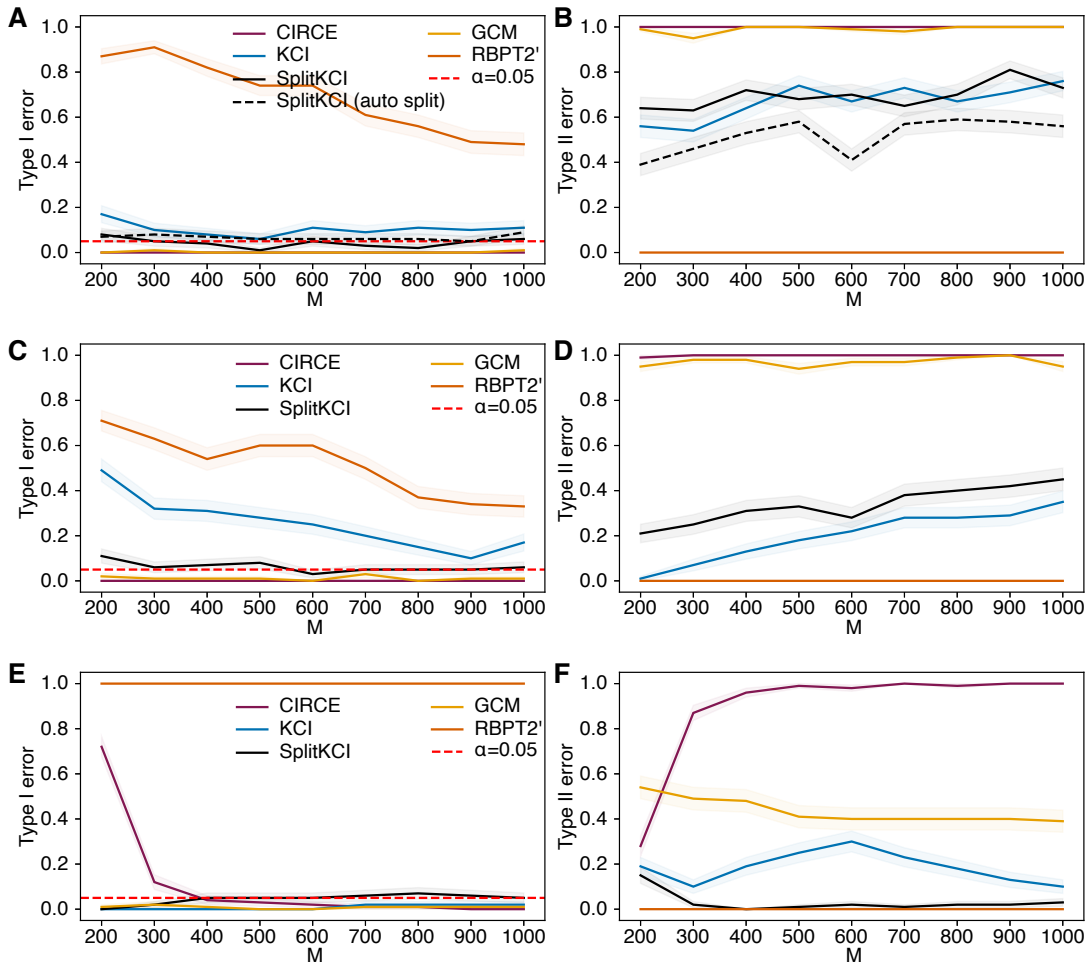


Figure 17: Synthetic neural data experiments for 400 (A, B, C) dataset size, but increasing amount of auxiliary (B, C) data. **A.** Type I error for 300/100 train/test split. **B.** Type II error. **C-D.** Same as A-B, but for 200/200 train/test split. **E-F.** Same as A-B, but without a train/test split. Lines/shaded area: mean/ \pm SE over 100 trials, $\alpha = 0.05$.

References

Mélisande Albert, Béatrice Laurent, Amandine Marrel, and Anouar Meynaoui. Adaptive test of independence based on hsic measures. *The Annals of Statistics*, 50(2):858–879, 2022.

Julia Angwin, Jeff Larson, Lauren Kirchner, and Surya Mattu. Minority neighborhoods pay higher car insurance premiums than white areas with the same risk. *ProPublica*, April 2017.

Mona Azadkia and Sourav Chatterjee. A simple measure of conditional dependence. *The Annals of Statistics*, 49(6):3070–3102, 2021.

Thomas B Berrett, Yi Wang, Rina Foygel Barber, and Richard J Samworth. The conditional permutation test for independence while controlling for confounders. *Journal of the Royal Statistical Society Series B: Statistical Methodology*, 82(1):175–197, 2020.

Felix Biggs, Antonin Schrab, and Arthur Gretton. MMD-FUSE: Learning and combining kernels for two-sample testing without data splitting. In *NeurIPS*, 2023.

Dean A Bodenham and Niall M Adams. A comparison of efficient approximations for a weighted sum of chi-squared random variables. *Statistics and Computing*, 26(4):917–928, 2016.

Emmanuel Candes, Yingying Fan, Lucas Janson, and Jinchi Lv. Panning for gold: ‘model-x’ knockoffs for high dimensional controlled variable selection. *Journal of the Royal Statistical Society Series B: Statistical Methodology*, 80(3):551–577, 2018.

Victor Chernozhukov, Denis Chetverikov, Mert Demirer, Esther Duflo, Christian Hansen, Whitney Newey, and James Robins. Double/debiased machine learning for treatment and structural parameters, 2018.

Kacper P Chwialkowski, Dino Sejdinovic, and Arthur Gretton. A wild bootstrap for degenerate kernel tests. In *NeurIPS*, 2014.

JJ Daudin. Partial association measures and an application to qualitative regression. *Biometrika*, 67(3):581–590, 1980.

Tamara Fernández and Nicolás Rivera. A general framework for the analysis of kernel-based tests, 2022.

Simon Fischer and Ingo Steinwart. Sobolev norm learning rates for regularized least-squares algorithms. *The Journal of Machine Learning Research*, 21(1):8464–8501, 2020.

Magalie Fromont, Béatrice Laurent, Matthieu Lerasle, and Patricia Reynaud-Bouret. Kernels based tests with non-asymptotic bootstrap approaches for two-sample problems. In *Conference on Learning Theory*, 2012.

Kenji Fukumizu, Francis R Bach, and Michael I Jordan. Dimensionality reduction for supervised learning with reproducing kernel hilbert spaces. *Journal of Machine Learning Research*, 5(Jan):73–99, 2004.

Kenji Fukumizu, Arthur Gretton, Xiaohai Sun, and Bernhard Schölkopf. Kernel measures of conditional dependence. In *NeurIPS*, volume 20, 2007.

Tom M George, Mehul Rastogi, William de Cothi, Claudia Clopath, Kimberly Stachenfeld, and Caswell Barry. RatInABox, a toolkit for modelling locomotion and neuronal activity in continuous environments. *eLife*, 13, February 2024. doi: 10.7554/elife.85274.

Arthur Gretton. Introduction to RKHS, and some simple kernel algorithms. Advanced Topics in Machine Learning lecture, University College London, 2013.

Arthur Gretton. A simpler condition for consistency of a kernel independence test. *arXiv preprint arXiv:1501.06103*, 2015.

Arthur Gretton, Olivier Bousquet, Alex Smola, and Bernhard Schölkopf. Measuring statistical dependence with Hilbert-Schmidt norms. In *ALT*, pages 63–77, 2005.

Arthur Gretton, Kenji Fukumizu, Choon Teo, Le Song, Bernhard Schölkopf, and Alex Smola. A kernel statistical test of independence. In *NeurIPS*, 2007.

Steffen Grünwald, Guy Lever, Luca Baldassarre, Sam Patterson, Arthur Gretton, and Massimilano Pontil. Conditional mean embeddings as regressors. In *ICML*, 2012.

Moritz Hardt, Eric Price, and Nathan Srebro. Equality of opportunity in supervised learning. In *Advances in Neural Information Processing Systems*, volume 29, 2016.

Z. Huang, N. Deb, , and B Sen. Kernel partial correlation coefficient — a measure of conditional dependence. *J. Mach. Learn. Res.*, 23(216):1–58, 2022.

Oscar Key, Arthur Gretton, Francois-Xavier Briol, and Tamara Fernandez. Composite goodness-of-fit tests with kernels. *arXiv preprint arXiv:2111.10275*, 2021.

Ilmun Kim and Antonin Schrab. Differentially private permutation tests: Applications to kernel methods. *arXiv preprint arXiv:2310.19043*, 2023.

Ilmun Kim, Matey Neykov, Sivaraman Balakrishnan, and Larry Wasserman. Local permutation tests for conditional independence. *The Annals of Statistics*, 50(6):3388–3414, 2022.

James J Knierim, Hemant S Kudrimoti, and Bruce L McNaughton. Place cells, head direction cells, and the learning of landmark stability. *Journal of Neuroscience*, 15(3): 1648–1659, 1995.

Anne Leucht and Michael H Neumann. Dependent wild bootstrap for degenerate U- and V-statistics. *Journal of Multivariate Analysis*, 117:257–280, 2013.

Yicheng Li, Haobo Zhang, and Qian Lin. On the saturation effect of kernel ridge regression. In *ICLR*, 2022a.

Zhu Li, Dimitri Meunier, Mattes Mollenhauer, and Arthur Gretton. Optimal rates for regularized conditional mean embedding learning. In *NeurIPS*, 2022b.

Zhu Li, Dimitri Meunier, Mattes Mollenhauer, and Arthur Gretton. Towards optimal Sobolev norm rates for the vector-valued regularized least-squares algorithm. *arXiv preprint arXiv:2312.07186*, 2023.

Zhu Li, Dimitri Meunier, Mattes Mollenhauer, and Arthur Gretton. Towards optimal sobolev norm rates for the vector-valued regularized least-squares algorithm. *Journal of Machine Learning Research*, 25(181):1–51, 2024.

Anton Rask Lundborg, Ilmun Kim, Rajen D Shah, and Richard J Samworth. The projected covariance measure for assumption-lean variable significance testing. *arXiv preprint arXiv:2211.02039*, 2022.

Afsaneh Mastouri, Yuchen Zhu, Limor Gultchin, Anna Korba, Ricardo Silva, Matt Kusner, Arthur Gretton, and Krikamol Muandet. Proximal causal learning with kernels: Two-stage estimation and moment restriction. In *ICML*, 2021.

Alec McClean, Sivaraman Balakrishnan, Edward H Kennedy, and Larry Wasserman. Double cross-fit doubly robust estimators: Beyond series regression. *arXiv preprint arXiv:2403.15175*, 2024.

Matey Neykov, Sivaraman Balakrishnan, and Larry Wasserman. Minimax optimal conditional independence testing. *The Annals of Statistics*, 49(4):2151–2177, 2021.

Junhyung Park and Krikamol Muandet. A measure-theoretic approach to kernel conditional mean embeddings. In *NeurIPS*, 2020.

Judea Pearl. *Causality: Models, Reasoning, and Inference*. Cambridge University Press, 2000.

Roman Pogodin, Namrata Deka, Yazhe Li, Danica J Sutherland, Victor Veitch, and Arthur Gretton. Efficient conditionally invariant representation learning. In *ICLR*, 2022.

Felipe Maia Polo, Yuekai Sun, and Moulinath Banerjee. Conditional independence testing under misspecified inductive biases. In *NeurIPS*, 2023.

Francesca Sargolini, Marianne Fyhn, Torkel Hafting, Bruce L McNaughton, Menno P Witter, May-Britt Moser, and Edvard I Moser. Conjunctive representation of position, direction, and velocity in entorhinal cortex. *Science*, 312(5774):758–762, 2006.

Meyer Scetbon, Laurent Meunier, and Yaniv Romano. An asymptotic test for conditional independence using analytic kernel embeddings. In *ICML*, 2022.

Cyrill Scheidegger, Julia Hörrmann, and Peter Bühlmann. The weighted generalised covariance measure. *The Journal of Machine Learning Research*, 23(1):12517–12584, 2022.

Antonin Schrab, Benjamin Guedj, and Arthur Gretton. KSD aggregated goodness-of-fit test. In *NeurIPS*, 2022a.

Antonin Schrab, Ilmun Kim, Benjamin Guedj, and Arthur Gretton. Efficient aggregated kernel tests using incomplete U -statistics. In *NeurIPS*, 2022b.

Antonin Schrab, Ilmun Kim, Mélisande Albert, Béatrice Laurent, Benjamin Guedj, and Arthur Gretton. MMD aggregated two-sample test. *Journal of Machine Learning Research*, 24(194):1–81, 2023.

Rajat Sen, Ananda Theertha Suresh, Karthikeyan Shanmugam, Alexandros G Dimakis, and Sanjay Shakkottai. Model-powered conditional independence test. In *NeurIPS*, 2017.

Rajen D Shah and Jonas Peters. The hardness of conditional independence testing and the generalised covariance measure. *The Annals of Statistics*, 48(3):1514–1538, 2020.

Xiaofeng Shao. The dependent wild bootstrap. *Journal of the American Statistical Association*, 105(489):218–235, 2010.

Shubhanshu Shekhar, Ilmun Kim, and Aaditya Ramdas. A permutation-free kernel independence test. *Journal of Machine Learning Research*, 24(369):1–68, 2023.

Hongjian Shi, Mathias Drton, and Fang Han. On azadkia–chatterjee’s conditional dependence coefficient. *Bernoulli*, 30(2):851–877, 2024.

Le Song, Alex Smola, Arthur Gretton, Karsten M Borgwardt, and Justin Bedo. Supervised feature selection via dependence estimation. In *ICML*, 2007.

Le Song, Jonathan Huang, Alex Smola, and Kenji Fukumizu. Hilbert space embeddings of conditional distributions. In *ICML*, 2009.

Peter Spirtes, Clark Glymour, and Richard Scheines. *Causation, Prediction, and Search*. Springer, 2nd edition, 2000.

Bharath Sriperumbudur, Kenji Fukumizu, and Gert Lanckriet. Universality, characteristic kernels and RKHS embedding of measures. *JMLR*, 12:2389–2410, 2011.

Ingo Steinwart and Clint Scovel. Mercer’s theorem on general domains: On the interaction between measures, kernels, and RKHSs. *Constructive Approximation*, 35:363–417, 2012.

Eric V Strobl, Kun Zhang, and Shyam Visweswaran. Approximate kernel-based conditional independence tests for fast non-parametric causal discovery. *Journal of Causal Inference*, 7(1):20180017, 2019.

Xiaohai Sun, Dominik Janzing, Bernhard Scholkopf, and Kenji Fukumizu. A kernel-based causal learning algorithm. In *ICML*, 2007.

Zoltán Szabó and Bharath K. Sriperumbudur. Characteristic and universal tensor product kernels. *Journal of Machine Learning Research*, 18(233):1–29, 2018.

Robert Tillman, Arthur Gretton, and Peter Spirtes. Nonlinear directed acyclic structure learning with weakly additive noise models. In *NeurIPS*, 2009.

Chien-Fu Jeff Wu. Jackknife, bootstrap and other resampling methods in regression analysis. *The Annals of Statistics*, 14(4):1261–1295, 1986.

Kun Zhang and Aapo Hyvärinen. On the identifiability of the post-nonlinear causal model. *arXiv preprint arXiv:1205.2599*, 2012.

Kun Zhang, Jonas Peters, Dominik Janzing, and Bernhard Schölkopf. Kernel-based conditional independence test and application in causal discovery. In *UAI*, 2011.